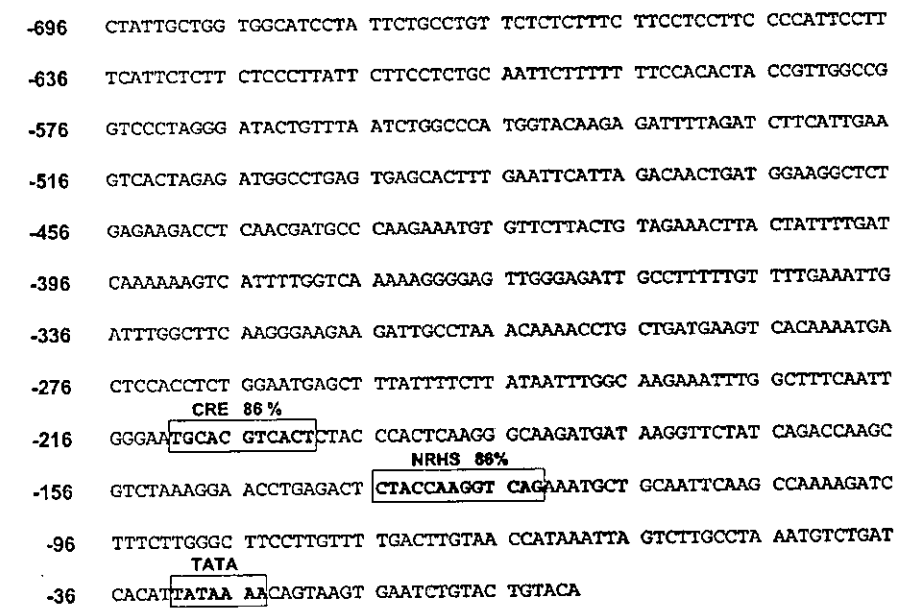

FIG. 1. The 5′-flanking region of the P450arom promoter II *cis*-acting elements are indicated in boxes. The percentages represent the degree of homology to consensus sequences of these DNA motifs. Please note that a CRE and a NRHS that binds SF-1 within the −517-bp flanking region are critical for baseline and cAMP-induced promoter activity.

by SF-1 via binding of SF-1 to a *cis*-acting element at −136/−124 bp upstream of P450arom gene promoter II (9). We also found that the −517/−215-bp region was essential for the most striking increases in baseline activity and cAMP fold-induction. SF-1 belongs to the orphan nuclear receptor family and regulates the expression of many steroidogenic genes in the adrenal and gonads via binding to nuclear receptor half site (NRHS) in their promoter regions. A number of regulators [*e.g.* steroid receptor coactivator-1, cAMP response element-binding protein, dosage-sensitive sex reversal adrenal hypoplasia congenita critical region on the X chromosome gene 1 (DAX-1), early growth response-1, sex-determining region Y-box 9, and Wilms' tumor suppressor gene (WT1)] interact with SF-1 to modify its transactivating functions (10–14).

DAX-1 is another member of the orphan nuclear receptor family (15, 16). DAX-1 is also expressed in the adrenal and gonads and shows a strikingly similar expression pattern to that of SF-1 (17, 18). This colocalization of SF-1 and DAX-1 led to the suggestion of a functional interaction between these two orphan nuclear receptors (17, 18). In fact, DAX-1-deficient male mice are infertile and have small testes (19). P450arom mRNA levels in testes and circulating estrogen levels are significantly increased in DAX-1-deficient mice due to the lack of inhibition on SF-1-mediated P450arom expression (20). DAX-1 has also been shown to repress SF-1-mediated transactivation of other steroidogenic genes, including genes for steroidogenic acute regulatory protein, 3β-hydroxysteroid dehydrogenase type II, Müllerian inhibiting substance (*MIS*), and P450c17 (*Cyp17*; Refs. 14 and 21–23).

The product of the WT1 contains a zinc finger domain and is essential for mammalian gonadal and kidney development (24). WT1 is highly conserved in mammalian species throughout the evolution. WT1 transcripts are present in a number of reproductive tissues including testicular Sertoli cells, ovarian granulosa cells, and endometrial stromal cells (25–28). *In vitro* and *in vivo* studies suggest that WT1 can act as a transcriptional repressor or activator (29, 30). WT1 was reported to regulate the transcription of the *MIS* gene by virtue of a protein-protein interaction with SF-1 (31). Alternative splicing of the WT1 gene generates four isoforms, all of which are expressed in WT1-positive tissues; the fifth exon may or may not be present, and an alternative splice site in intron 9 allows the addition of three amino acids (Lys-Thr-Ser, or KTS) between the third and fourth zinc fingers of the WT1 protein (32). WT1(−KTS) isoform was reported to be more potent than the +KTS isoform in the stimulation of the *MIS* gene promoter (14).

In view of these observations, we have examined the modulation of cAMP/SF-1-mediated human P450arom gene expression by WT1 and DAX-1 in endometriotic and endometrial cells. We also studied differential expression and possible *in vivo* roles of WT1 and DAX-1 in endometriosis and normal endometrium. We should also point out that this is the first report demonstrating the regulation of aromatase expression by WT1 in any cell type or species.

Materials and Methods

Tissue acquisition and processing

Cyst walls of ovarian endometriomas (n = 8, 5 proliferative and 3 luteal phase samples dissected from surrounding tissue under microscope) and eutopic endometrial tissues (n = 14) were processed to culture stromal cells using a protocol previously described by Ryan *et al.* with minor modifications (33). Eight of the eutopic endometrial samples for stromal cell cultures were obtained at the time of surgical removal of the ovarian endometriomas. The remaining six endometrial samples were obtained from endometriosis-free women undergoing hysterectomy for cervical intraepithelial neoplasia (three proliferative and three luteal phase samples). Extraovarian endometriosis and eutopic endometrial tissue biopsies for immunohistochemistry were obtained simultaneously from another group of women (n = 6) undergoing laparoscopy for endometriosis during both proliferative and luteal phases, as confirmed via histological analysis. The age range of the patient population was 23–45 yr.

Stromal cell culture methodology was described previously (7, 33).

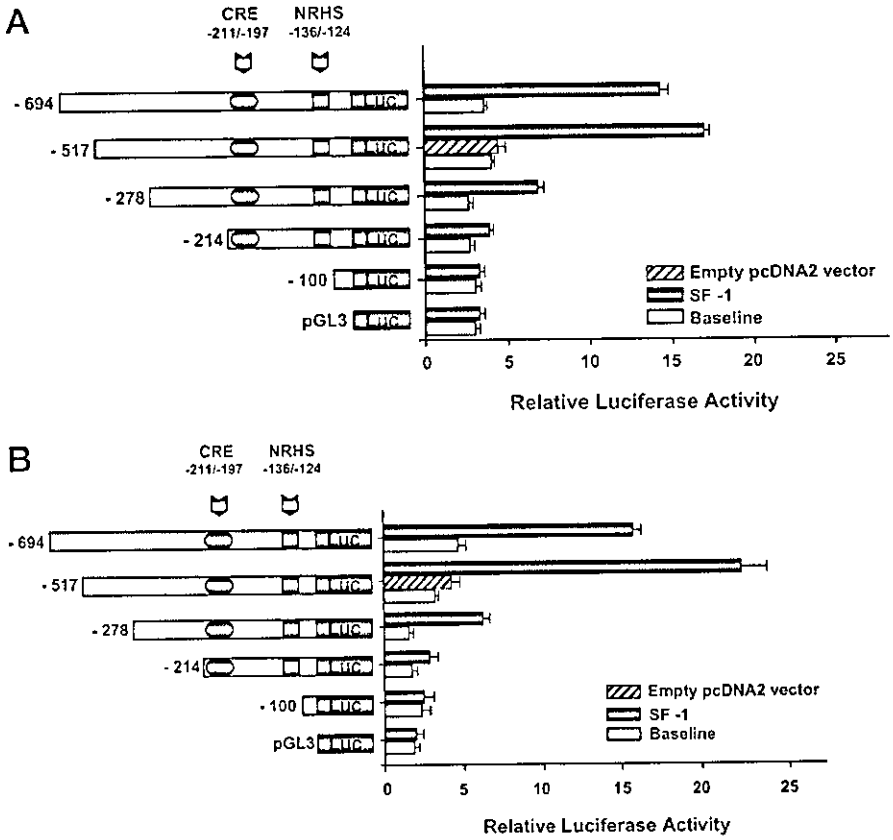

FIG. 2. Identification of regulatory regions responsible for SF-1-mediated P450arom promoter II activity in human endometrial and endometriotic stromal cells. Reporter plasmids containing the 5′-flanking region of the human P450arom gene with deletion mutations are represented on the *left*. Relative positions and sequences of the imperfect CRE (−211/−197 bp) and the NRHS (−136/−124 bp) are indicated. Luciferase plasmids containing the 5′-flanking region of human P450arom promoter II with serial deletions (−100, −214, −278, −517, and −694 bp) were transfected with or without SF-1 expression vector into human endometrial (A) and endometriotic stromal cells (B). Please note that the fold-induction by SF-1 in endometriotic cells was more pronounced compared with endometrial cells.

Briefly, endometrial or endometriotic tissues were rinsed with sterile saline solution, minced finely, and digested with collagenase B (1 mg/ml) and deoxyribonuclease (0.1 mg/ml) at 37 C for 30–60 min. Stromal cells were then suspended in DMEM/F-12 1:1 10% fetal bovine serum (FBS; Life Technologies, Inc./BRL, Grand Island, NY). Fresh suspensions of these cells were plated in 35-mm culture dishes at a cell density of 50,000/cm^2 and kept in an incubator in a humidified atmosphere with 5% CO_2 at 37 C. Twelve to 24 h after the attachment of stromal cells, culture medium was removed and cells were washed twice with DMEM/F-12. Then, cells were maintained in DMEM/F-12 containing 10% FBS. Medium was changed at 48 h intervals until the cells became confluent. Human tissues were collected as per a research protocol and informed consent approved by the Institutional Review Board of the University of Illinois at Chicago.

Plasmid constructs and site-directed mutagenesis

Human SF-1 cDNA (~3.1 kb) in the eukaryotic expression vector pcDNA2 was a generous gift from Drs. Meera Ramayya and Keith L. Parker (UT Southwestern Medical Center at Dallas, Dallas, TX). Human DAX-1 cDNA (~1.5 kb) in the expression vector pBKCMV was a generous gift from Dr. J. Larry Jameson (Northwestern University, Chicago, IL). Mouse wt1 cDNA (with or without KTS domains) in pcDNA3.1 vectors were generous gifts from Dr. Daniel A. Haber (Harvard Medical School, Boston, MA). Preparation of the deletion mutants of the *CYP19* (P450arom) gene 5′-flanking sequence in pGL3-basic luciferase vector has been described previously (34). Generation of the −517/−16-bp luciferase plasmid bearing a mutation in the −136/−124-bp SF-1 binding motif has also been described previously (Fig. 1) (34). Briefly, the NRHS (−136/−124 bp) sequence was changed from 5′-ACCAGGTCAGAAA-3′ to 5′-ACCcccTCAGAAA-3′; using the GeneEditor *in vitro* site-directed mutagenesis system (Promega Corp., Madison, WI), as per the manufacturer's instructions. (The lowercase nucleotides indicate the mutations.) The mutations and the orientation of insert were confirmed by direct sequencing. Plasmids used in transfection experiments were purified using an EndoFree Plasmid Isolation Kit (QIAGEN, Valencia, CA), and their purity was verified by spectrophotometry and agarose gel electrophoresis.

Transient transfections and luciferase assays

Primary endometrial and endometriotic stromal cells were transfected using Lipofectamine Plus (Life Technologies, Inc.-BRL) with the following plasmids: 1) 0.5 μg of deletion or mutant constructs of P450arom promoter II cloned into pGL3-basic luciferase reporter plasmids; 2) 0.5 μg of pcDNA3 or 0.3 μg pBKCMV expression plasmid (Invitrogen, Carlsbad, CA), containing the cDNAs encoding SF-1, and WT1 or DAX-1; and 3) *Renilla* luciferase (5 ng, Promega Corp.) employed as an internal control for transfection efficiency. Total DNA transfected per well was kept at a constant total of 2 μg/well, adding empty pcDNA3 vector if necessary. The day before transfection, primary stromal cells were seeded into 35-mm dishes at 2 × 10^5 cell/dish. At the time of transfection, stromal cells were 80% confluent. The transfection solution was made of 200 μl of Opti-MEM reduced-serum medium containing PLUS reagent (6 μl), precomplexed DNA, and 4 μl of Lipofectamine reagent. After transfection for 3 h in transfection solution at 37 C in 5% CO_2, medium was changed to antibiotic-free DMEM/F-12 containing 10% FBS for overnight recovery. Cells were then kept in serum-free medium for 12 h. Thereafter, cells in serum-free medium were treated with 0.5 mM dibutyryl cAMP (Bt_2cAMP) for 24 h. After treatment, transfected cells were washed twice in PBS and lysed in 250 μl luciferase lysis buffer (0.1 M potassium phosphate, pH 7.8, 1% Triton X-100, 1 mM dithiothreitol, 2 mM ethylenediaminotetraacetic acid. Luciferase and *Renilla* luciferase readings were obtained using a dual-luciferase reporter assay system (Promega Corp.), and LUMAT LB9507 luminometer (Berthold Technologies GmbH & Co. KG, Bad Wildbad, Germany).

Results are presented as the mean ± SEM of data from triplicate

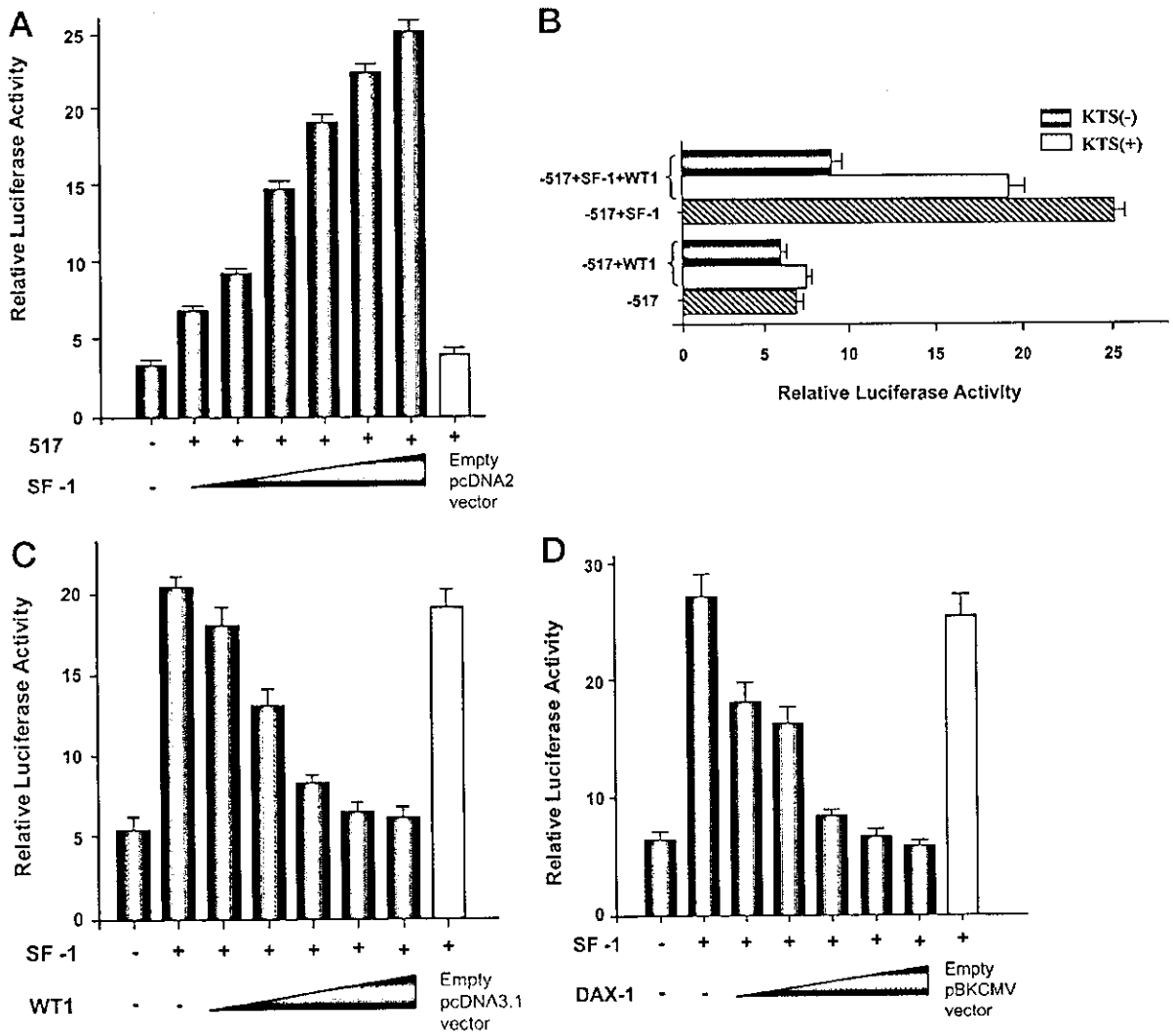

FIG. 3. SF-1 induces, whereas WT1 and DAX-1 down-regulate, P450arom promoter II activity in primary endometrial stromal cells in a dose-dependent manner. Luciferase plasmids containing the −517-bp 5′-flanking region of human P450arom promoter II were cotransfected with increasing amounts (10–1000 ng) of SF-1 (A), WT1 (C), and/or DAX-1 (D) expression vectors into endometrial stromal cells. B, The relative potencies of WT1 isoforms (−KTS *vs.* +KTS) in the down-regulation of P450arom promoter II activity.

replicates. Illustrated results are representative of five reproducible experiments using cells from five different patients.

Immunohistochemistry

Mouse monoclonal antibody against human WT1 (recognizing an amino-terminal epitope of human origin) and rabbit polyclonal antibody against DAX-1 (recognizing an amino-terminal epitope of DAX-1 of human origin) were purchased from Santa Cruz Biotechnology, Inc. (Santa Cruz, CA). The immunohistochemical procedures were performed, as previously described, using the biotin-streptavidin amplified technique with a histone immunostaining kit (Nichirei, Tokyo, Japan). Antigen retrieval was performed by heating the slides in an autoclave at 120 C for 5 min in citric acid buffer (2 mM citric acid and 9 mM trisodium citrate dehydrate, pH 6.0). The dilutions of the primary antibodies used in this study were 1:1250 for WT1 and 1:500 for DAX-1. The antigen-antibody complex was visualized with 3.3′-diaminobenzidine solution (0.01 M 3.3′-diaminobenzidine in 0.05 M Tris-HCl buffer, pH 7.6; and 0.006% hydrogen peroxide) and counterstained with hematoxylin. Human tissues of kidney and adrenal gland were used as positive controls for WT1 and DAX-1 antibodies, respectively. As negative controls, normal mouse or rabbit IgG was used instead of the primary antibodies. No specific immunoreactivity was detected in these sections.

The immunoreactivity was quantified by an H-scoring system as originally described by McCarty *et al.* (35) with modifications. H-scores were generated by adding together 2× percentage of strongly stained nuclei in 10 high power fields and 1× percentage of weakly stained nuclei in 10 high power field giving a range from 0–200 (36). WT1 or DAX-1 staining was observed exclusively in nuclei, as expected.

Statistical analysis

A two-tailed *t* test and Bonferroni correction were used to compare the means of H-scores for WT1 and DAX-1 in stromal and epithelial cells of endometrium and endometriosis. Because we performed multiple *t* tests between these groups (Table 2), α-value for each individual test after Bonferroni correction was 0.01274. This brought the overall α-level to 0.05.

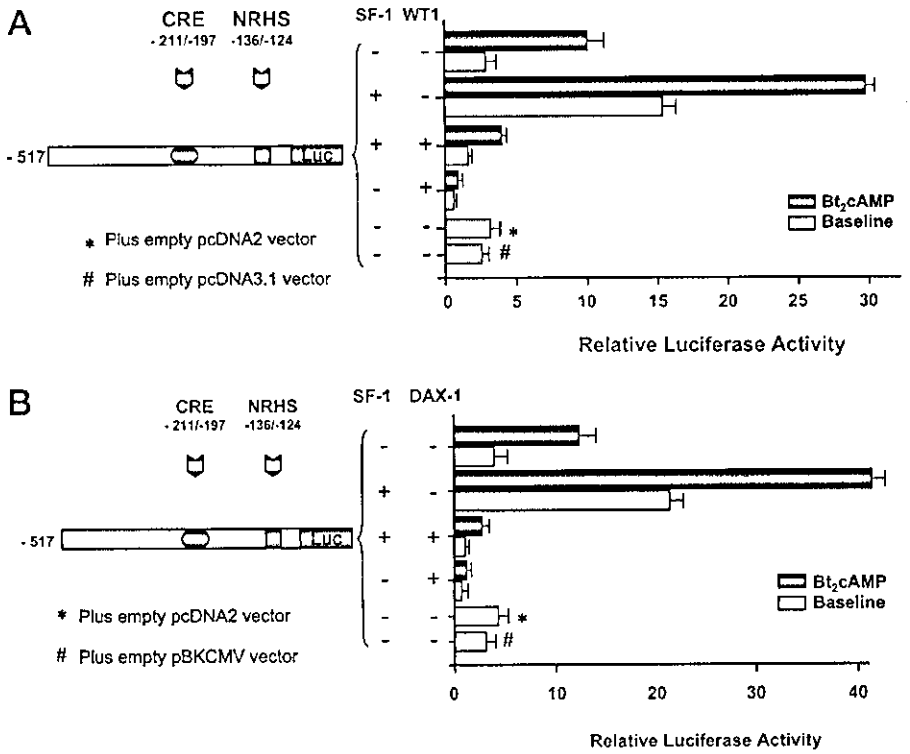

FIG. 4. The effects of WT1 and DAX-1 on the activity of −517-bp promoter II construct in endometriotic stromal cells. Mammalian expression vectors, SF-1 and WT1 (A) and SF-1 and DAX-1 (B) were cotransfected into endometriotic stromal cells in various combinations. Ectopic expression of SF-1 (500 ng) and/or treatment with Bt_2cAMP stimulated promoter II activity. WT1 (250 ng) and DAX-1 (250 ng) decreased or abolished SF-1-mediated or Bt_2cAMP-stimulated activity of the −517-bp promoter II construct in endometriotic stromal cells.

Results

Regulatory sequences in P450 promoter II that confer SF-1-mediated transcription in endometrial and endometriotic stromal cells

To identify regions of the P450arom promoter II that are responsible for SF-1-mediated transcription of the P450arom gene in endometrial and endometriotic stromal cells, we first transfected serial deletion mutants of P450arom promoter II into these cells. Plasmids containing −100, −214, −278, −517, and −694 bp regions of the promoter II fused to the luciferase reporter gene were transfected into endometrial and endometriotic stromal cells in culture. These cells were cultured in the absence of serum or hormone, with or without human SF-1 expression vector. SF-1 induced the luciferase activity of −214 bp (but not the −100 bp) promoter II plasmids by 1.4-fold in endometrial stromal cells. The addition of SF-1 to −278, −517, −694 bp luciferase plasmid in endometrial stromal cells gave rise to 2.3-, 4-, and 3.6-fold inductions, respectively (Fig. 2A). These results indicate that the proximal region between −214 and −100 bp conferred minimal responsiveness to SF-1 in endometrial stromal cells, and that this was markedly potentiated by the −517/−214-bp region. The NRHS (−136/−124 bp) and cAMP response element (CRE; −211/−197 bp) in the −214/−140-bp region have been shown to be functionally important previously (Fig. 1) (9, 37, 38).

The promoter activity profile of deletion mutants in endometriotic stromal cells was similar to that observed in endometrial cells (Fig. 2B). Fold-induction by SF-1 in endometriotic cells, however, was more pronounced (2-, 3.4-, 7-, and 4-fold for −214, −278, −517, and −694 bp construct, respectively) compared with those in endometrial cells (Fig. 2B). This was suggestive of a more efficient transcriptional machinery favoring binding of stimulatory factors and possible deficiency of factors that inhibit P450arom promoter II in endometriotic *vs.* endometrial cells.

WT1 or DAX-1 down-regulate SF-1-induced transcriptional activation of P450arom promoter II gene in a dose-dependent manner in endometrial stromal cells

Previous studies have demonstrated the roles of SF-1 in transcriptional activation of human P450arom gene and DAX-1 in the transcriptional repression of murine *Cyp19* gene (9, 20, 38). WT1 and DAX-1 have been shown to independently modify SF-1-mediated gene transcription of *MIS* via direct interaction with SF-1 (14). The role of DAX-1 in the regulation of the human P450arom gene or WT1 in the regulation of the P450arom gene in any species, however, has not been reported to date. We therefore studied the effects of WT1 and DAX-1 on SF-1-mediated stimulation of the human P450arom promoter II activity by transfecting mammalian expression plasmids.

The effects of WT1 and DAX-1 on P450arom promoter II activity were dose-dependent (Fig. 3). We first demonstrated that SF-1-induced promoter activity in a dose-dependent fashion, as expected (Fig. 3A). Then, we assessed the effect of WT1 isoforms with or without a KTS domain on SF-1-mediated P450arom promoter II activity (Fig. 3B). WT1(−KTS) is much more potent than WT1(+KTS) in the suppression of SF-1-induced P450arom promoter activity (Fig. 3B). The addition of WT1(−KTS) effectively decreased SF-1-induced promoter II activity in a dose-dependent man-

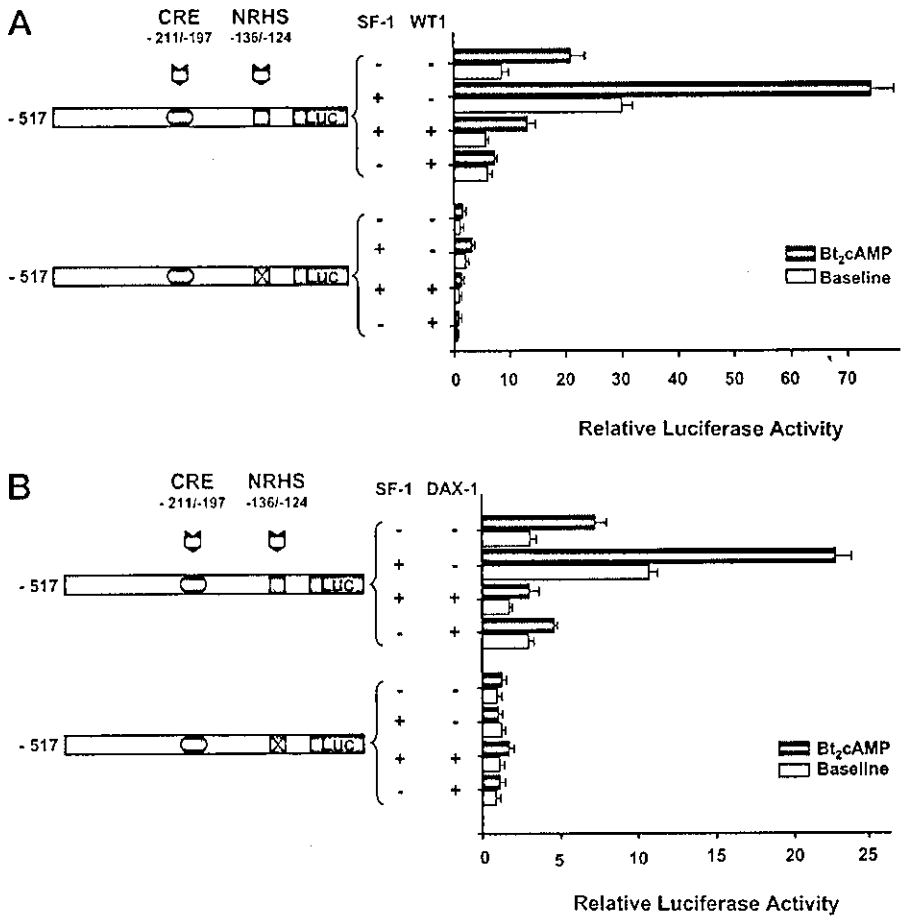

FIG. 5. Disruption of NRHS and the effects of WT1 and DAX-1 on the activity of −517-bp promoter II construct in endometrial stromal cells. The NHRS at −136/−124 bp is critical for aromatase expression in endometriosis, because disruption of this site abolished or decreased promoter II activity in endometrial stromal cells. A, Mammalian expression vectors, SF-1 (500 ng) and WT1 (250 ng) were cotransfected into endometrial stromal cells, together with either the wild-type −517 or $-517^{\Delta-136/-124}$ bp promoter II construct. Ectopic expression of SF-1 and treatment with Bt_2cAMP-stimulated promoter II activity of the wild-type −517-bp construct but not that of the $-517^{\Delta-136/-124}$ bp promoter II construct, whereas WT1 abolished both SF-1-mediated and cAMP-induced activity. B, The effects of DAX-1 (250 ng) on the activity of the −517-bp promoter II construct in endometrial stromal cells. Cotransfection of SF-1 and/or DAX-1 expression vectors together with the wild-type or mutant promoter II construct showed a similar pattern observed in A.

ner (Fig. 3C). DAX-1 also inhibited SF-1-mediated promoter II activity in a dose-dependent fashion (Fig. 3D).

WT1 or DAX-1 down-regulates SF-1-mediated P450arom promoter II transcription in endometriotic stromal cell line

After investigating the roles of SF-1, WT1, and DAX-1 in the regulation of P450arom promoter II in endometrial cell line, we next sought to determine the roles of these factors in the regulation of P450arom in endometriotic stromal cells. Figure 4, A and B, shows the effects of ectopically expressed SF-1, WT1, or DAX-1 on the activity of −517 bp promoter II construct in Bt_2cAMP-treated endometriotic stromal cells. SF-1 significantly increased P450arom transcription in endometriotic stromal cell, whereas either WT1 or DAX-1 markedly reduced promoter II activity. Hence, our results suggest that WT1 or DAX-1 may play an important role in the regulation of P450arom expression in the human endometriotic stromal cells.

The sequence (−136/−124 bp) is important for the regulation of P450arom promoter II by SF-1, WT1, and DAX-1

To better understand the functions of the *cis*-acting element NRHS at −136/−124 bp, we introduced a disruptive mutation at this site in the −517-bp construct and determined its effects on promoter activity. First, we observed that Bt_2cAMP potentiated promoter II activity in the presence or absence of SF-1 using the wild-type construct. The disruption of the −136/−124-bp NRHS significantly decreased both baseline and SF-1-induced promoter II activity in endometrial stromal cells (Fig. 5, A and B). In view of our previous data demonstrating dominant binding of SF-1 to the NRHS at −136/−124 bp, we suggest that the interaction of SF-1 with this site is critical for P450arom promoter II activity in endometrial stromal cells (9).

The addition of SF-1 to endometrial stromal cells gave rise to significant increases in baseline and Bt_2cAMP-induced promoter II activity (Fig. 5, A and B). The addition of WT1 to endometrial stromal cells decreased the baseline and Bt_2cAMP-induced promoter activity in the presence or absence of SF-1, suggesting that WT1 inhibits promoter II activity mediated by an interaction of SF-1 with the −136/−124-bp NRHS (Fig. 5A). On the other hand, disruption of the −136/−124-bp NRHS totally abolished promoter II activity regardless of the presence of SF-1, Bt_2cAMP, or WT1 (Fig. 5A).

The addition of DAX-1 also inhibited SF-1 or Bt_2cAMP-mediated induction of promoter II activity (Fig. 5B). As in the

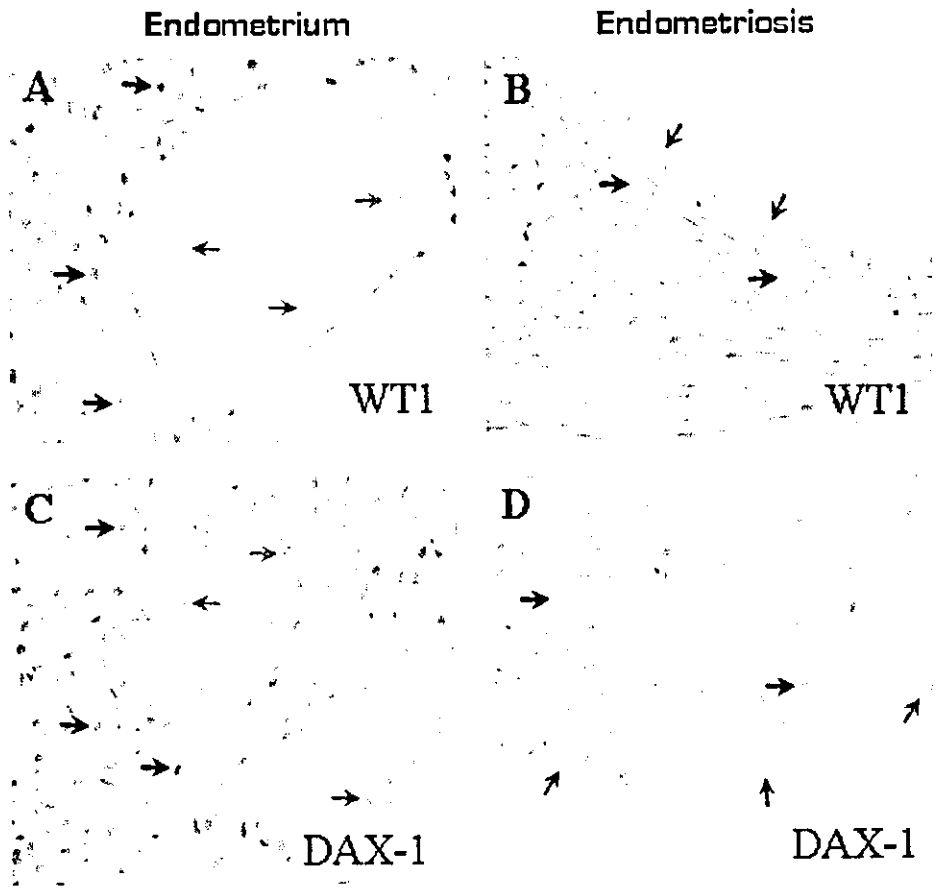

FIG. 6. Distribution of WT1 and DAX-1 in endometrial and endometriotic tissues *in situ*. The *in vivo* presence of WT1 and DAX-1 were verified in simultaneously obtained eutopic endometrial (endometrium) and endometriotic (endometriosis) tissues. Both epithelial (*blue arrows*) and stromal (*black arrows*) cells demonstrated nuclear immunoreactivity for WT1 and DAX-1. WT1 was predominantly observed in stromal cells of the endometrium (A). Endometriotic stromal cells, on the other hand, contained significantly lesser quantities of immunoreactive WT1 (B). DAX-1 immunoreactivity was readily detectable in both stromal and epithelial cells of endometrium (C) and endometriosis (D). We quantified immunoreactivity of WT1 and DAX-1 in both tissues by H-scoring and applied statistical analysis (Tables 1 and 2).

TABLE 1. Immunohistochemistry scores in simultaneously biopsied endometrium and endometriosis samples

Patients	Phase	Cell type	Endometrium H-Score		Endometriosis H-Score	
			WT1	DAX-1	WT1	DAX-1
1	Luteal	Epithelium	6	173	2	146
		Stroma	42	72	18	131
2	Luteal	Epithelium	6	138	11	149
		Stroma	73	142	24	155
3	Proliferative	Epithelium	21	133	11	144
		Stroma	66	103	21	94
4	Luteal	Epithelium	22	188	4	106
		Stroma	63	86	30	72
5	Proliferative	Epithelium	8	86	4	83
		Stroma	58	66	52	106
6	Luteal	Epithelium	6	183	6	114
		Stroma	22	133	53	122

case of WT1, site-directed mutagenesis suggests that the stimulatory effect of SF-1 and the inhibitory effect of DAX-1 on P450arom promoter II activity were at least in part mediated by the −136/−124-bp NRHS (Fig. 5, A and B).

In vivo distribution of WT1 and DAX-1 in endometrial and endometriotic tissues

Cellular distribution and levels of WT1 and DAX-1 were evaluated by immunohistochemistry in endometrial and endometriotic tissue using the human anti-WT1 and DAX-1 antibodies (Santa Cruz Biotechnology, Inc.). In four luteal and two proliferative endometrial tissues and simultaneously obtained extraovarian endometriotic implants, WT1 and DAX-1 were detected in various cell types of the majority of the samples (Fig. 6).

Immunoreactive WT1 was readily detectable in endometriotic stromal cells, whereas WT1 immunointensity was markedly less in endometriotic stromal cells (Fig. 6, A and B). Interestingly, endometrial or endometriotic epithelial cells contained strikingly less WT1 compared with stromal cells. DAX-1, on the other hand, was readily detected in both endometrial and endometriotic epithelial and stromal cells (Fig. 6, C and D).

We used a semiquantitative H-scoring system to compare WT1 and DAX-1 immunointensity between the cell types represented in Fig. 6. When endometrium and endometriosis

TABLE 2. Statistical analysis of levels of WT1 and DAX-1 in simultaneously biopsied endometrium and endometriosis samples

Endometrium	Mean score (n = 6)	Endometriosis	Mean score (n = 6)	Two-tailed *t* test
WT1				
Epithelium[(1)]	14.8 ± 9.1	Epithelium[(2)]	6.3 ± 3.8	$P_{(1-2)} = 0.06362$
Stroma[(3)]	65.0 ± 15.3	Stroma[(4)]	33.0 ± 15.6	$P_{(3-4)} = 0.00528^a$
DAX-1				
Epithelium[(5)]	150.16 ± 38.9	Epithelium[(6)]	123.66 ± 26.8	$P_{(6-6)} = 0.17364$
Stroma[(7)]	100.33 ± 31.6	Stroma[(8)]	113.33 ± 29.1	$P_{(7-8)} = 0.43654$

[a] Significant for α, 0.01274 after Bonferroni correction. Because multiple *t* tests were performed, α-value for each test after Bonferroni correction was 0.01274. This brought the overall α-level to 0.05.

$P_{(1-3)} = 0.00004^a$; $P_{(2-4)} = 0.03342$; $P_{(5-7)} = 0.03543$; $P_{(6-8)} = 0.53256$.

were compared, a statistically significant difference was observed only between endometriotic and endometrial stromal cells with respect to WT1 (Tables 1 and 2). Endometriotic stromal WT1 levels were significantly lower than those in endometrial stromal cells (Table 2). Moreover, we found that WT1 is expressed in significantly higher levels in stromal (*vs.* epithelial) cells in endometrium. We also observed a similar trend in endometriosis, although this did not reach statistical significance (Table 2). No statistically significant differences between epithelial and stromal cells were observed with respect to DAX-1 expression, although a trend for preferential expression in the epithelium was observed (Table 2).

Discussion

This study was performed to determine molecular mechanisms responsible for the modulation of aromatase expression by SF-1, WT1, and DAX-1 in endometrial and endometriotic stromal cells. We previously showed that significantly increased SF-1 in endometriotic *vs.* endometrial stromal cells represents a critical mechanism for aromatase expression and estrogen production in endometriosis (9). Binding of SF-1 to the critical −136/−124-bp element (NRHS) in P450arom promoter II may be the key event that brings the entire transcriptional complex to initiate P450arom expression in endometriosis. Chicken ovalbumin upstream promoter-transcription factor (COUP-TF), on the other hand, is present in both endometriosis and endometrium and inhibits aromatase expression in the absence of SF-1 in endometrium (9). SF-1 serves as a dominant activator for P450arom promoter II via competing with COUP-TF for binding to the NRHS at −136/−124 bp in cultured endometriotic stromal cells (9). This competition between SF-1 and COUP-TF, however, is not sufficient to explain aberrant aromatase expression in endometriosis, because 20% of eutopic endometrial samples also expressed the dominant activator SF-1; yet these tissues did not contain aromatase in levels comparable to those in endometriosis. Thus, there may be other fail-safe mechanisms in addition to COUP-TF for ensuring the suppression of aromatase expression in endometrium.

Our present findings regarding the predominant expression of WT1 in endometrial *vs.* endometriotic cells and dominant repressor effect of WT1 on P450arom promoter II are strongly suggestive that WT1 serves as a physiologically important inhibitor of aromatase in the eutopic endometrium. Previously published data regarding stromal expression of WT1 in the endometrium are supportive of our findings (28).

Significantly decreased WT1 expression in endometriosis is interesting in view of recently implicated roles of other tumor suppressors in endometriosis. It was proposed that mutations of the tumor suppressor genes p53 and phosphatase and tensin homolog might play important roles in the etiology of endometriosis (39, 40). There are, however, conflicting data in the literature regarding the possible roles of these tumor suppressors in endometriosis (41, 42). To date, no definitive mechanisms have been shown for tumor suppressors in the pathogenesis of endometriosis. We demonstrate, for the first time, the down-regulation of a tumor suppressor, namely, WT1 in endometriosis. Moreover, we uncover one of the functions of WT1, namely suppression of estrogen production in endometrium. Studies are currently under way to understand whether aromatase inhibition is a general function of WT1 in other human tissues.

DAX-1 shows profiles of expression and function similar to those of COUP-TF. In other words, DAX-1 is ubiquitously expressed in both endometrium and endometriosis and down-regulates aromatase. DAX-1 may represent another fail-safe mechanism for the inhibition of aromatase in normal endometrium.

Acknowledgments

We thank Meera Ramayya, Keith L. Parker (UT Southwestern Medical Center at Dallas), J. Larry Jameson (Northwestern University), and Daniel A. Haber (Harvard Medial School) for the generous gifts of human SF-1 cDNA, human DAX-1 cDNA, and mouse wt1 cDNA, respectively.

Received April 2, 2002. Accepted May 23, 2002.

Address all correspondence and requests for reprints to: Serdar E. Bulun, M.D, Department of Obstetrics and Gynecology, University of Illinois at Chicago, 820 South Wood Street, M/C808, Chicago, Illinois 60612. E-mail: sbulun@uic.edu.

This work was supported by the National Institutes of Health Grant HD38691 (to S.E.B.).

References

1. Vessey MP, Villard-Mackintosh L, Painter R 1993 Epidemiology of endometriosis in women attending family planning clinics. BMJ 306:182–184
2. Kjerulff KH, Erickson BA, Langenberg PW 1996 Chronic gynecological conditions reported by US women: findings from the National Health Interview Survey, 1984 to 1992. Am J Public Health 86:195–199
3. Olive DL, Schwartz LB 1993 Endometriosis. N Engl J Med 328:1759–1769
4. Dizerega GS, Barber DL, Hodgen GD 1980 Endometriosis: role of ovarian steroids in initiation, maintenance, and suppression. Fertil Steril 33:649–653
5. Simpson ER, Mahendroo MS, Means GD, Kilgore MW, Hinshelwood MM, Graham-Lorence S, Amarneh B, Ito Y, Fisher CR, Michael MD 1994 Aromatase cytochrome P450, the enzyme responsible for estrogen biosynthesis. Endocr Rev 15:342–355
6. Noble LS, Simpson ER, Johns A, Bulun SE 1996 Aromatase expression in endometriosis. J Clin Endocrinol Metab 81:174–179

7. **Noble LS, Takayama K, Zeitoun KM, Putman JM, Johns DA, Hinshelwood MM, Agarwal VR, Zhao Y, Carr BR, Bulun SE** 1997 Prostaglandin E2 stimulates aromatase expression in endometriosis-derived stromal cells. J Clin Endocrinol Metab 82:600–606
8. **Takayama K, Zeitoun K, Gunby RT, Sasano H, Carr BR, Bulun SE** 1998 Treatment of severe postmenopausal endometriosis with an aromatase inhibitor. Fertil Steril 69:709–713
9. **Zeitoun K, Takayama K, Michael MD, Bulun SE** 1999 Stimulation of aromatase P450 promoter (II) activity in endometriosis and its inhibition in endometrium are regulated by competitive binding of steroidogenic factor-1 and chicken ovalbumin upstream promoter transcription factor to the same *cis*-acting element. Mol Endocrinol 13:239–253
10. **Monte D, DeWitte F, Hum DW** 1998 Regulation of the human P450scc gene by steroidogenic factor 1 is mediated by CBP/p300. J Biol Chem 273:4585–4591
11. **Ito M, Yu R, Jameson JL** 1997 DAX-1 inhibits SF-1-mediated transactivation via a carboxy-terminal domain that is deleted in adrenal hypoplasia congenita. Mol Cell Biol 17:1476–1483
12. **Halvorson LM, Ito M, Jameson JL, Chin WW** 1998 Steroidogenic factor-1 and early growth response protein 1 act through two composite DNA binding sites to regulate luteinizing hormone β-subunit gene expression. J Biol Chem 273: 14712–14720
13. **De Santa Barbara P, Bonneaud N, Boizet B, Desclozeaux M, Moniot B, Sudbeck P, Scherer G, Poulat F, Berta P** 1998 Direct interaction of SRY-related protein SOX9 and steroidogenic factor 1 regulates transcription of the human anti-Mullerian hormone gene. Mol Cell Biol 18:6653–6665
14. **Nachtigal MW, Hirokawa Y, Enyeart-VanHouten DL, Flanagan JN, Hammer GD, Ingraham HA** 1998 Wilms' tumor 1 and Dax-1 modulate the orphan nuclear receptor SF-1 in sex-specific gene expression. Cell 93:445–454
15. **Zanaria E, Muscatelli F, Bardoni B, Strom TM, Guioli S, Guo W, Lalli E, Moser C, Walker AP, McCabe ER, Meitinger T, Monaco AP, Sassone-Corsi P, Camerino G** 1994 An unusual member of the nuclear hormone receptor superfamily responsible for X-linked adrenal hypoplasia congenita. Nature 372:635–641
16. **Swain A, Zanaria E, Hacker A, Lovell-Badge R, Camerino G** 1996 Mouse Dax1 expression is consistent with a role in sex determination as well as in adrenal and hypothalamus function. Nat Genet 12:404–409
17. **Guo W, Burris TP, McCabe ER** 1995 Expression of DAX-1, the gene responsible for X-linked adrenal hypoplasia congenita and hypogonadotropic hypogonadism, in the hypothalamic-pituitary-adrenal/gonadal axis. Biochem Mol Med 56:8–13
18. **Ikeda Y, Swain A, Weber TJ, Hentges KE, Zanaria E, Lalli E, Tamai KT, Sassone-Corsi P, Lovell-Badge R, Camerino G, Parker KL** 1996 Steroidogenic factor 1 and Dax-1 colocalize in multiple cell lineages: potential links in endocrine development. Mol Endocrinol 10:1261–1272
19. **Yu RN, Ito M, Jameson JL** 1998 The murine Dax-1 promoter is stimulated by SF-1 (steroidogenic factor-1) and inhibited by COUP-TF (chicken ovalbumin upstream promoter-transcription factor) via a composite nuclear receptor-regulatory element. Mol Endocrinol 12:1010–1022
20. **Wang ZJ, Jeffs B, Ito M, Achermann JC, Yu RN, Hales DB, Jameson JL** 2001 Aromatase (*Cyp19*) expression is up-regulated by targeted disruption of Dax1. Proc Natl Acad Sci USA 98:7988–7993
21. **Zazopoulos E, Lalli E, Stocco DM, Sassone-Corsi P** 1997 DNA binding and transcriptional repression by DAX-1 blocks steroidogenesis. Nature 390: 311–315
22. **Lalli E, Melner MH, Stocco DM, Sassone-Corsi P** 1998 DAX-1 blocks steroid production at multiple levels. Endocrinology 139:4237–4243
23. **Hanley NA, Rainey WE, Wilson DI, Ball SG, Parker KL** 2001 Expression profiles of SF-1, DAX1, and CYP17 in the human fetal adrenal gland: potential interactions in gene regulation. Mol Endocrinol 15:57–68
24. **Park S, Bernard A, Bove KE, Sens DA, Hazen-Martin DJ, Garvin AJ, Haber DA** 1993 Inactivation of WT1 in nephrogenic rests, genetic precursors to Wilms' tumour. Nat Genet 5:363–367
25. **Pelletier J, Schalling M, Buckler AJ, Rogers A, Haber DA, Housman D** 1991 Expression of the Wilms' tumor gene WT1 in the murine urogenital system. Genes Dev 5:1345–1356
26. **Zhou J, Rauscher 3rd FJ, Bondy C** 1993 Wilms' tumor (WT1) gene expression in rat decidual differentiation. Differentiation 54:109–114
27. **Charles AK, Mall S, Watson J, Berry PJ** 1997 Expression of the Wilms' tumour gene WT1 in the developing human and in paediatric renal tumours: an immunohistochemical study. Mol Pathol 50:138–144
28. **Makrigiannakis A, Coukos G, Mantani A, Prokopakis P, Trew G, Margara R, Winston R, White J** 2001 Expression of Wilms' tumor suppressor gene (WT1) in human endometrium: regulation through decidual differentiation. J Clin Endocrinol Metab 86:5964–5972
29. **Lee TH, Moffett P, Pelletier J** 1999 The Wilms' tumor suppressor gene (WT1) product represses different functional classes of transcriptional activation domains. Nucleic Acids Res 27:2889–2897
30. **Menke AL, van der Eb AJ, Jochemsen AG** 1998 The Wilms' tumor 1 gene: oncogene or tumor suppressor gene? Int Rev Cytol 181:151–212
31. **Lee SB, Haber DA** 2001 Wilms tumor and the WT1 gene. Exp Cell Res 264:74–99
32. **Haber DA, Sohn RL, Buckler AJ, Pelletier J, Call KM, Housman DE** 1991 Alternative splicing and genomic structure of the Wilms tumor gene WT1. Proc Natl Acad Sci USA 88:9618–9622
33. **Ryan IP, Schriock ED, Taylor RN** 1994 Isolation, characterization, and comparison of human endometrial and endometriosis cells *in vitro*. J Clin Endocrinol Metab 78:642–649
34. **Zhou J, Gurates B, Yang S, Sebastian S, Bulun SE** 2001 Malignant breast epithelial cells stimulate aromatase expression via promoter II in human adipose fibroblasts: an epithelial-stromal interaction in breast tumors mediated by CCAAT/enhancer binding protein β. Cancer Res 61:2328–2334
35. **McCarty Jr KS, Miller LS, Cox EB, Konrath J, McCarty Sr KS** 1985 Estrogen receptor analyses. Correlation of biochemical and immunohistochemical methods using monoclonal antireceptor antibodies. Arch Pathol Lab Med 109:716–721
36. **Suzuki T, Takahashi K, Darnel AD, Moriya T, Murakami O, Narasaka T, Takeyama J, Sasano H** 2000 Chicken ovalbumin upstream promoter transcription factor II in the human adrenal cortex and its disorders. J Clin Endocrinol Metab 85:2752–2757
37. **Michael MD, Kilgore MW, Morohashi K, Simpson ER** 1995 Ad4BP/SF-1 regulates cyclic AMP-induced transcription from the proximal promoter (PII) of the human aromatase P450 (*CYP19*) gene in the ovary. J Biol Chem 270: 13561–13566
38. **Michael MD, Michael LF, Simpson ER** 1997 A CRE-like sequence that binds CREB and contributes to cAMP-dependent regulation of the proximal promoter of the human aromatase P450 (*CYP19*) gene. Mol Cell Endocrinol 134: 147–156
39. **Bischoff FZ, Simpson JL** 2000 Heritability and molecular genetic studies of endometriosis. Hum Rep Update 6:37–44
40. **Bayramaoglu H, Duzcan E** 2001 Atypical epithelial changes and mutant p53 gene expression in ovarian endometriosis. Pathol Oncol Res 7:33–38
41. **Nakayama K, Toki T, Zhai YL, Lu X, Horiuchi A, Nikaido T, Konishi I, Fujii S** 2001 Demonstration of focal p53 expression without genetic alterations in endometriotic lesions. Int J Gynecol Pathol 20:227–231
42. **Schneider J, Jimenez E, Rodriguez F, del Tanago JG** 1998 c-myc, c-erb-B2, nm23 and p53 expression in human endometriosis. Oncol Rep 5:49–52

TOXICOLOGICAL SCIENCES 81, 273–279 (2004)
doi:10.1093/toxsci/kfh241
Advance Access publication July 28, 2004

No-observed Effect Levels for Carcinogenicity and for *in vivo* Mutagenicity of a Genotoxic Carcinogen

Manabu Hoshi,*,† Keiichirou Morimura,* Hideki Wanibuchi,* Min Wei,* Eriko Okochi,‡ Toshikazu Ushijima,‡ Kunio Takaoka,† and Shoji Fukushima*,[1]

*Department of Pathology, Osaka City University Medical School, 1-4-3 Asahi-machi, Abeno-ku, Osaka 545-8585, Japan; †Department of Orthopaedic Surgery, Osaka City University Medical School, 1-4-3 Asahi-machi, Abeno-ku, Osaka 545-8585, Japan; and ‡Carcinogenesis Division, National Cancer Center Research Institute, 1-1, Tsukiji, 5 chome, Chuo-ku, Tokyo 104-0045, Japan

Received April 14, 2004; accepted June 10, 2004

To elucidate the relationship between *in vivo* carcinogenic and mutagenic potentials of genotoxic carcinogens, low doses were tested in the livers of Big Blue transgenic rats with 2-amino-3,8-dimethylimidazo[4,5-*f*]quinoxaline (MeIQx). Male Big Blue rats were fed a diet containing 0.001, 0.01, 0.1, 1, 10, or 100 ppm of MeIQx for 16 weeks, and the frequencies of *lacI* mutants and glutathione *S*-transferase placental form (GST-P) positive foci in the liver were determined. The mutation frequencies significantly increased at doses of 10 and 100 ppm, and GST-P positive foci significantly increased at a dose of 100 ppm. However, no statistical increases in both frequencies were observed at lower doses. MeIQx most frequently induced G frameshifts, followed by G to T transversions. Thus, no observed effect level (NOEL) was demonstrated for both carcinogenicity in terms of preneoplastic lesion induction and *in vivo* mutagenicity of MeIQx, and the NOEL for *in vivo* mutagenicity was lower than that for carcinogenicity.

Key Words: MeIQx; no-observed effect level; *in vivo* mutagenicity; carcinogenicity.

More than 80% of human cancers may be related to carcinogenic environmental chemicals (Doll and Peto, 1981). Carcinogenicity is generally detected by long-term carcinogenicity testing in rodents using doses considerably in excess of human exposure levels. The situation is complicated by the fact that carcinogens can be classified as either genotoxic or non-genotoxic according to results of *in vitro* genotoxicity tests. The currently accepted view is that no threshold exists for the carcinogenic potential of genotoxic carcinogens, with the response curve approaching zero in a linear fashion with extrapolation from the doses used in carcinogenicity testing (Preussmann, 1980). Actual human cancer risk of genotoxic carcinogens is very difficult to assess, because few directly obtained data are available from the carcinogenicity testing at low doses such as human daily exposure levels (Truhaut, 1979). Therefore, practical information concerning cancer risk remains inadequate, and the need for investigation in this field is urgent.

A heterocyclic amine produced in the cooking of meat and fish, 2-amino-3,8-dimethylimidazo[4,5-*f*]quinoxaline (MeIQx), is a potent genotoxic carcinogen that shows strong mutagenicty in the Ames assay (Johansson and Jagerstad, 1994; Sugimura, 1986). MeIQx is metabolized *in vivo* to N-hydroxyamino derivatives by cytochrome P450 and then activated by the esterification enzymes, acetyltransferase and sulfotransferase. The activated form produces DNA adducts, particularly involving guanine bases, which can lead to mutations (Langouet *et al.*, 2001). MeIQx induces hepatocellular carcinomas in male rats with exposure at high doses (Kato *et al.*, 1988; Kushida *et al.*, 1994) and also glutathione *S*-transferase placental form (GST-P)-positive foci, well-established preneoplastic lesions in the livers of rats which have been accepted as end-points for assessing carcinogenic potential in the liver in medium-term bioassay (Ito *et al.*, 1988).

Somatic mutation is considered responsible for carcinogenesis with stepwise accumulation of alterations in cancer-related genes leading to malignant neoplasia (Vogelstein and Kinzler, 1993). DNA damage and irreversible DNA base change appear to play an important role in this multiple-step carcinogenesis. The Big Blue transgenic rodent mutagenesis assay is used widely for *in vivo* mutagenicity assays, and the reliability of this system has been established (Kohler *et al.*, 1991). The system originally was designed to assess DNA damage *in vivo* in a tissue-specific manner. We have used the rats in this system to determine both mutagenic and carcinogenic potentials of test substances in the same individual animal.

Our group recently showed no increase in quantitative data for GST-P-positive foci in liver on treatment of rats with very low doses of MeIQx, indicating the existence of a threshold for carcinogenicity (Fukushima, *et al.*, 2002, 2003). Mutagenicity remained at issue, however (Solomon *et al.*, 1996) and *in vitro* mutagenicity tests of genotoxic carcinogens generally show DNA damage to be dose-dependent in a truly linear manner (Maier and Schawalder, 1988). Therefore, a discrepancy may

[1] To whom correspondence should be addressed. Fax: +81-6-6646-3093. E-mail: fukuchan@med.osaka-cu.ac.jp.

exist between *in vivo* carcinogenic and *in vitro* mutagenic potential. However, little information is available concerning *in vivo* mutagenicity of genotoxic carcinogens, especially at low doses.

As the first step toward to elucidating the mechanism of MeIQx-induced mutagenicity, it is necessary to establish suitable target genes as biomarkers in the field of genotoxicology. Most genotoxic carcinogens may exert not only carcinogenicity but also *in vivo* mutagenicity in an organ specific manner but this aspect has not been hitherto explored in detail. Few background data on susceptibility of non-target organs to induction of mutations by chemical carcinogens have been generated (Nishikawa *et al.*, 1997). Therefore, there is further need for investigation at the whole body level, including target and non-target organs after treatment with genotoxic carcinogens and for identification of the tissue-specificity of *in vivo* mutagenicity, compared to its carcinogenicity.

In the present study, to determine *in vivo* carcinogenicity and mutagenicity from treatment with MeIQx at low doses representing human exposure levels, we used a rodent mutagenesis system together with a medium-term liver carcinogenicity test, which we employed previously for low dose carcinogenicity of rats (Fukushima *et al.*, 2002). At high doses, *in vivo* mutagenicity was examined for multiple organ systems.

MATERIALS AND METHODS

Chemicals. The carcinogen, MeIQx (purity, 99.9%), was obtained from Nard Institute (Nishinomiya, Japan).

Animals and treatments. A total of 40 Big Blue male rats with genetic background of Fisher 344 were purchased from Stratagene (La Jolla, CA) at the age of 4–5 weeks. The animals were divided into seven groups, receiving MeIQx at doses of 0 ppm (group 1, control), 0.001 ppm (group 2), 0.01 ppm (group 3), 0.1 ppm (group 4), 1 ppm (group 5), 10 ppm (group 6), and 100 ppm (group 7) in powdered basal diet (Oriental MF, Oriental Yeast, Co., Ltd., Tokyo, Japan) continuously for 16 weeks after an acclimation period of one week. The lowest level, 0.001 ppm of MeIQx, was established as equivalent to the daily intake of this carcinogen in humans (IARC, 1993). MeIQx diets were prepared by Oriental Yeast Co., Ltd. and the MeIQx concentration in each was confirmed by high-performance liquid chromatography (HPLC). Group 1 comprised 10 rats, while groups 2 to 7 included 5 rats each. The animals were housed two or three to a plastic cage with paper chips for bedding under constant conditions (room temperature, 22 ± 2°C; relative humidity, 55.5%; light/dark cycle, 12:12 h). Body weights, food consumption, and water intake were recorded weekly.

Collection of tissue samples. Upon completion of MeIQx treatment or basal diet alone, the rats were killed under ether anesthesia for removal of livers for mutation analysis and immunohistochemical examination to detect GST-P-positive foci and proliferating cell nuclear antigen (PCNA). Formalin-fixed, paraffin-embedded liver tissue (three sections from each of left lateral lobe, medial lobe, and the right lateral lobe) was either routinely stained with hematoxylin and eosin (H&E) or immunohistochemically stained for GST-P-positive foci or PCNA positive cells. Remaining unfixed liver tissues were quickly frozen in liquid nitrogen and kept frozen at −80°C until DNA isolation.

For multiple organ analysis, Big Blue rats at the age of 4–5 weeks were employed. They were divided into two groups of five animals each receiving MeIQx at doses of 0 and 100 ppm continuously for 16 weeks. The rats were sacrificed and liver, colon, Zymbal gland, kidney, spleen, lung, testis, heart, brain, fat tissue, and skeletal muscle of quadriceps femoris were collected. Formalin-fixed samples of skeletal muscle of brain, liver, lung, testis, kidney, spleen, and heart, were routinely embedded in paraffin wax for staining of sections with hematoxylin and eosin. The remaining tissues were quickly frozen in liquid nitrogen and kept frozen −80°C until DNA isolation.

Plaque color screening assay. High-molecular-weight genomic DNA was extracted by the phenol/chloroform extraction methods, and phages were recovered using a Transpack Packaging Extract (Stratagene, CA) (Rogers *et al.*, 1995). Mutation frequency in *lacI* gene was analyzed by the method recommended by Stratagene (Okochi *et al.*, 1999; Suzuki *et al.*, 1996a). Phages from each fully blue plaque were stored in 500 µl of SM buffer (0.1 M NaCl, 8 mM $MgSO_4$, 50 mM Tris-HCl at pH 7.5, and 0.01% gelatin) with 50 µl of chloroform at 4°C. For analysis of the *lacI* gene, blue plaques were isolated and replated at low density on X-gal containing NZYM agar plates to confirm the mutant plaque. The mutant phages were independently collected in SM buffer containing 10% chloroform for direct sequencing.

DNA sequencing of mutant lacI. Direct sequencing was performed with an ABI PRISM 3100 Genetic Analyzer (PE Applied Biosystems. Chiba, Japan). The DNA sequences of all mutants isolated from the livers of control and MeIQx-treated rats were analyzed with designed primers (Ushijima *et al.*, 1995). Mutations were classified into three categories: single base substitution, frameshift, and others. When a base pair deletion mutation occurred in the same nucleotide, the nucleotide with the lowest number was assigned as the mutation site.

Immunohistochemical detection of GST-P-positive foci and PCNA. Immunohistochemical detection of GST-P-positive foci was performed by the avidin-biotin-peroxidase complex (ABC) method described previously (Kitano *et al.*, 1998). Foci comprising two or more positive hepatocytes were counted under a light microscope. Total areas of sections were measured using a color image processor (IPAP Sumika Technos, Osaka, Japan), and numbers of foci per square centimeter of liver tissue were calculated by a well-trained pathologist. Proliferating epithelial cells ratio were detected with anti-PCNA antibody staining (DAKO Japan, Kyoto, Japan), also using the ABC method.

Statistical analysis. Statistical analysis of the observed values was performed using the Student's *t*-test. All calculations were performed with the aid of the Stat View statistical package (Abacus Concepts, Inc., Berkeley, CA). Significance of differences between the expected and the observed values of mutation frequencies and GST-P positive foci were analyzed using Super ANOVA Duncan New Multiple Range analysis.

RESULTS

Final Body Weights, Liver Weights, Total Intakes of MeIQx, and Histological Examination

Final body weights, liver weights, and total intakes of MeIQx are shown in Table 1. All rats survived in good condition until the scheduled time, 16 weeks, for liver examination, and no adverse effects were observed in rats treated with MeIQx at various doses. No statistically significant differences were found between groups with regard to body or liver weights. Likewise, food consumption and water intake did not differ (data not shown). Average total MeIQx intakes in each group were dose-dependent. No obvious macroscopic or microscopic changes, including tumors, were detected in the liver, colon, Zymbal gland, kidney, spleen, lung, testis, heart, brain, fat tissue, and skeletal muscle of quadriceps femoris of any rat.

In vivo *Mutagenicity at Low-Dose Treatment of MeIQx*

For the *in vivo* mutagenesis assay at low doses, data for total plaque forming units, mutation-containing-plaque forming

TABLE 1
Final Body Weights, Liver Weights, and Total MeIQx Intakes

Group	MeIQx dose (ppm)	No. of rats	Final body weights (g)	Liver: Absolute (g)	Liver: Relative to body (%)	Total MeIQx intake (μg/rat/day)
1	0	10	420 ± 17	13.8 ± 0.7	3.3 ± 0.2	0
2	0.001	5	413 ± 19	13.7 ± 0.4	3.3 ± 0.1	0.0172
3	0.01	5	418 ± 11	13.5 ± 0.6	3.2 ± 0.1	0.1706
4	0.1	5	420 ± 13	13.4 ± 0.4	3.2 ± 0.1	1.73
5	1	5	428 ± 25	13.4 ± 0.9	3.1 ± 0.1	18.26
6	10	5	413 ± 30	13.7 ± 1.5	3.3 ± 0.1	174.3
7	100	5	410 ± 17	14.0 ± 0.6	3.4 ± 0.1	1738

Note. Values are mean ± SD. MeIQx, 2-amino-3,8-dimethylimidazo[4,5-*f*] quinoxaline.

TABLE 2
Mutation Frequency of *LacI* and GST-P Positive Foci in Liver

Group	MeIQx dose (ppm)	Total PFU	Mutant PFU	Mutation frequency ($/10^6$)	GST-P positive foci (no./cm^2)
1	0	1212518	18	14.8 ± 7.6	0.43 ± 0.53
2	0.001	598230	9	14.9 ± 12.2	0.18 ± 0.20
3	0.01	582621	9	15.6 ± 9.6	0.31 ± 0.68
4	0.1	588001	12	19.9 ± 17.5	0.33 ± 0.38
5	1	566516	17	29.4 ± 21.7	0.19 ± 0.26
6	10	565055	29	51.4 ± 14.2*	0.78 ± 0.49
7	100	616449	396	641.5 ± 176.9*	7.46 ± 1.77*

Note. Values are mean ± SD. MeIQx, 2-amino-3,8-dimethylimidazo[4,5-*f*] quinoxaline; GST-P, glutathione S-transferase placental form; PFU, plaque forming unit.
*$p < 0.001$ vs. group 1.

units, and calculated mutation frequencies are shown in Table 2. Mutation frequency in the liver of the control group treated without MeIQx was 14.8 ± 7.6, and mutation frequencies in groups treated with 1 ppm and less were not significantly different from that of the control group. Values for 10 and 100 ppm MeIQx groups were significantly increased compared with the control group frequency. The *in vivo* mutagenic dose-response curve of mutation frequency at low doses did not parallel the MeIQx dose (Fig. 1A).

Carcinogenicity at Low-Dose Treatment of MeIQx

Numbers of GST-P-positive foci in the liver did not differ significantly from those in the control group at 10 ppm and less (Table 2). Only foci in animals receiving the 100 ppm treatment were significantly increased beyond control-group numbers. The *in vivo* carcinogenic dose-response curve in terms of numbers of GST-P-positive foci did not parallel MeIQx doses (Fig. 1B).

PCNA-Positive Cells

PCNA-positive cells were counted to quantify cell proliferative ratio in the liver. PCNA-positive liver cells per 1500 hepatocytes were expressed as percentages. No significant differences were observed between MeIQx treatments and control groups (Fig. 2). Thus, the hepatocyte-proliferation rate was similar in all groups. Furthermore, with the highest dose no significant differences were detected between MeIQx-treated and control groups in the various organs, Zymbal gland, kidney, spleen, lung, testis, heart, brain, and skeletal muscle (data not shown).

In vivo *Mutagenicity at High-Dose Treatment of MeIQx*

Data for total plaque forming units (pfu), mutated pfu, and calculated mutation frequency for the multiple organs in the high dose experiment are shown in Table 3. The administration of MeIQx (five mice) significantly increased *lacI* mutation frequency in the liver ($p < 0.0001$), Zymbal gland ($p = 0.0078$), and colon ($p = 0.006$), compared to the control (five rats). Especially in the liver, mutation frequency was extremely elevated. On the other hand, no statistically significant elevation of the *lacI* mutation frequency was observed in the kidney, spleen, lung, testis, heart, brain, fat tissue, and skeletal muscle, lung, kidney, spleen, testis, brain, heart and fat tissue.

LacI *Sequence Analysis*

The results of sequence analysis of 150 MeIQx-treated group and two control group liver mutated blue plaques are shown in Table 4. The most frequent mutation type in the MeIQx-treated group was the frameshift (60.0%), followed by base substitution (32.0%). The most frequent mutation was 1 bp GC deletions (48.0%), followed by GC to TA transversion (26.7%) and then 2 bp GC deletions (9.3%). The two spontaneous mutations were a GC to AT transition and a T insertion. CpG sites were involved in 55.3% of the liver mutations.

DISCUSSION

The present study disclosed new aspects of carcinogenic and *in vivo* mutagenic properties of the genotoxic carcinogen, MeIQx. Dose-response curves for induction of GST-P positive foci and *in vivo* mutagenicity in liver were nonlinear in the region near zero. Thus, NOEL was demonstrated not only for carcinogenicity but also for *in vivo* mutagenicity at low doses. The NOEL for *in vivo* mutagenicity was lower than that for carcinogenicity.

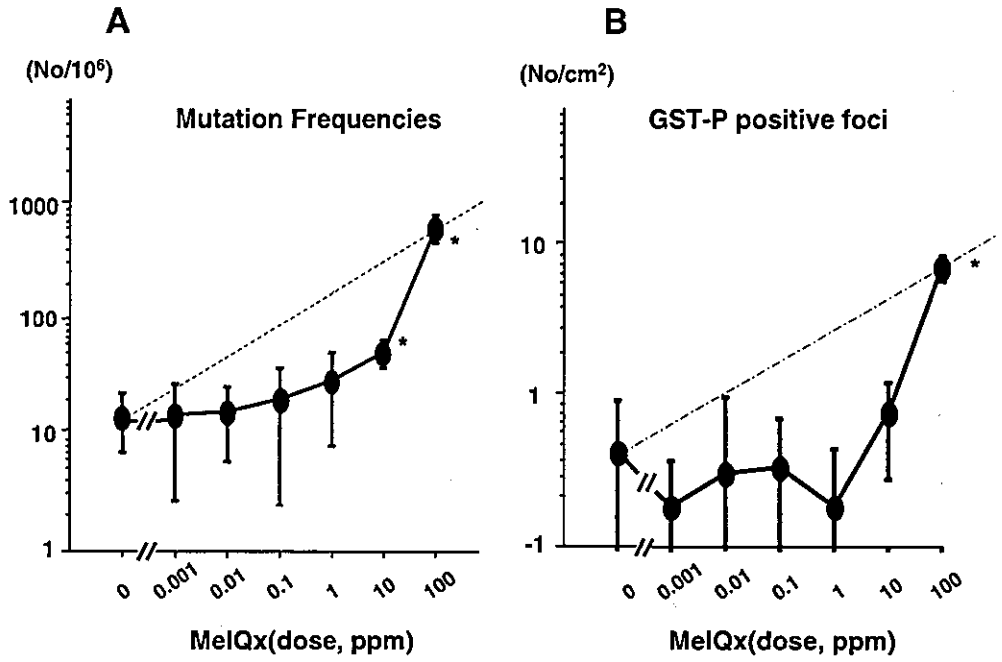

FIG. 1. Mutation frequencies (A) and GST-P-positive foci in the liver (B). Mutation frequencies of groups treated with 1 ppm and less MeIQx demonstrate no significant difference from the control group. In contrast, the values for 10 and 100 ppm MeIQx groups are significantly increased. The numbers of GST-P positive foci of groups treated with 10 ppm and less similarly demonstrate no statistically significant difference from the controls, only the value for the 100 ppm-treated group being significantly increased. *$p < 0.001$ vs. control. Broken lines (A, B) represent dose-response linear lines, which are predicted from two points at doses of 0 and 100 ppm.

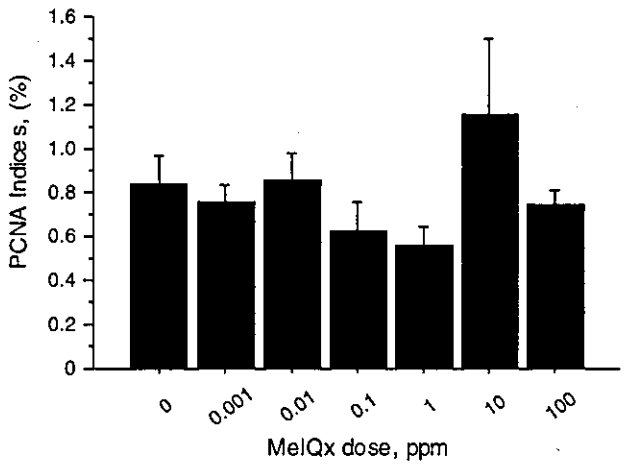

FIG. 2. PCNA indices in the liver. The cell proliferation indices do not differ significantly between the groups. Columns show means; Bars show SD.

Absence of a threshold for carcinogenicity of genotoxic carcinogens has long been assumed because, even when low doses of carcinogen do not induce tumors in rodents, genotoxic carcinogens are considered capable of damaging DNA at any exposure level, ultimately resulting in a tumor causing (Lutz, 1998). However, the present *in vivo* data disagree with the assumption.

To support non-linearity of dose-response curve induced by MeIQx treatment, we compared our non-linear curve of mutation frequency and GST-P positive foci to presumptive dose-response linear curve. Assuming linearity of dose-response for at low dose extrapolating from high dose, we could represent the dose-response linear line of mutation frequency from two points at dose of 0 and 100 ppm in this report. Herein, cancer risk per ppm (6.26/ppm) could be calculated from 641.5 ± 14.8 per 100 ppm (Fig. 1A). At 10 ppm one would expect a frequency of $14.8 + 6.26 \times 10 = 77.4$, compared to the observed value of 51.4 ± 14.2; at 1 ppm $14.8 + 6.26 \times 1 = 21.1$, compared to the observed value of 29.4 ± 21.7, samely, at 0.1 ppm $14.8 + 0.626 =$ 15.4, compared to the observed value of 19.9 ± 17.5, at 0.01 ppm $14.8 + 0.06 = 14.9$, compared to the observed value of 15.6 ± 9.6, at 0.001 ppm $14.8 + 0.006 = 14.8$, compared to the observed value of 14.9 ± 12.2. This assumption of the dose–response linear line was also applied to the data of GST-P positive foci (Fig. 1B). The expected numbers were 1.13 at 10 ppm, 0.50 at 1 ppm, 0.44 at 0.1 ppm, 0.43 at 0.01 ppm, 0.43 at 0.001 ppm, compared to the observed value of 0.78 ± 0.49, 0.19 ± 0.26, 0.33 ± 0.38, 0.31 ± 0.68, 0.18 ± 0.20, respectively, at each dose. For analysis of relationship between the expected and our

TABLE 3
LacI Mutation Frequency in Big Blue Rat

Organ	Treatment	No. of rats	Total plaques	Mutants	MF ($/10^6$)	*p* value
Liver						
	Control	5	597954	2	3.6 ± 4.9	<0.0001
	MeIQx (100 ppm)	5	824139	150	187.1 ± 46.3	
Colon						
	Control	5	669478	10	14.7 ± 10.2	0.0078
	MeIQx (100 ppm)	5	645073	45	70.9 ± 34.2	
Zymbal gland						
	Control	5	525882	9	17.3 ± 14.7	0.006
	MeIQx (100 ppm)	5	554359	25	45.0 ± 8.0	
Kidney						
	Control	5	727196	3	4.5 ± 4.3	0.0502
	MeIQx (100 ppm)	5	582432	18	29.9 ± 24.3	
Spleen						
	Control	5	613333	3	7.8 ± 8.9	0.0743
	MeIQx (100 ppm)	5	585557	15	26.0 ± 17.7	
Lung						
	Control	5	771305	12	15.9 ± 10.8	0.2726
	MeIQx (100 ppm)	5	791231	21	27.1 ± 19.1	
Testis						
	Control	5	618023	4	6.5 ± 9.0	0.6
	MeIQx (100 ppm)	5	668661	3	4.2 ± 3.8	
Heart						
	Control	5	618498	11	18.1 ± 15.9	0.317
	MeIQx (100 ppm)	5	688995	22	30.1 ± 19.4	
Brain						
	Control	5	544099	7	13.0 ± 8.1	0.2405
	MeIQx (100 ppm)	5	869835	7	8.0 ± 3.0	
Fat tissue						
	Control	5	529914	1	1.8 ± 3.9	0.2946
	MeIQx (100 ppm)	5	614889	3	4.8 ± 4.5	
Skeletal muscle						
	Control	5	782761	5	5.8 ± 8.2	0.686
	MeIQx (100 ppm)	5	519045	2	3.9 ± 5.4	

Note. MF, mutation frequency.

TABLE 4
Mutation Spectra of *LacI* in Liver

	Control		MeIQx	
	n	%	*n*	%
Single base substitution				
Transversion				
GC → TA			40	26.7
GC → CG			2	1.3
AT → TA			5	3.3
AT → CG			1	0.7
Total				32.0
Transition				
GC → AT	1	50	8	5.3
AT → GC			2	1.3
Total				6.7
Frameshift				
Single base deletion				
G			72	48.0
T			2	1.3
Two base deletion				
GC			14	9.3
Single base insertion				
A			1	0.7
T	1	50		
Two base insertion				
AA			1	0.7
Total				60.0
Others				
G → CT			1	0.7
TG → AT			1	0.7
Total				1.4
(at CpG sites			83	55.3)
Total	2	100	150	100

observed value of mutation frequencies and GST-P positive foci, these data was statistically calculated. Concerning the mutation frequencies, the significance ($p < 0.05$) was found at dose of 10 ppm, and the others were not. Concerning the value of GST-P positive foci, no significance was found at any dose.

Genotoxic carcinogens including MeIQx can induce DNA damage and fixation to result in potentially carcinogenic mutations (Langouet *et al.*, 2001). While specific cancer-related genes targeted by MeIQx have not been identified, if the 30 to 40 copies of *lacI* genes inserted into chromosome 4 in Big Blue rats are randomly affected by genotoxic carcinogens, they can serve as a marker of overall genetic instability in the presence of a mutagen. Thus, we studied mutation frequency of the *lacI* gene as a surrogate for cancer-related genes.

According to our results, NOEL of genetoxic carcinogens may exist at low doses, at which many adaptive and/or defensive responses within the organism may work to maintain biologic homeostasis. Metabolic pathways for detoxification, immune responses, cytokines, scavenger systems, hormones, and up-regulation of suppressor genes may play important roles (Lutz, 2001). Apoptosis, as well as DNA repair mechanisms by which altered bases are removed from DNA and replaced with the correct base, could counteract low level damage to DNA (Oesch *et al.*, 2000). In radiation carcinogenesis, especially at low doses, such biologic adaptive responses have been reported (Wolff, 1998), and defenses against low doses of chemical carcinogens may be similar.

In estimation of the carcinogenic influence of genotoxic carcinogens, DNA adducts are useful markers for examination for exposure assessment (Bailey *et al.*, 1994; Troxel *et al.*, 1997). However, this method does not represent demonstration of a carcinogenic effect, since DNA adduct formation does not always result in actual mutations. Moreover, MeIQx-DNA adducts can be detected in rat liver in a dose-dependent manner (Yamashita *et al.*, 1990), with small but apparent effects at low doses which are not in agreement with the exhibited threshold for carcinogenic potential at low doses (Fukushima *et al.*, 2003).

Cell proliferation must be considered for understanding mechanisms of chemical carcinogenesis (Cohen and Ellwein, 1990), since DNA alterations induced in cancer-related genes can influence cell growth. We presently used immunohistochemistry for PCNA to estimate cell proliferative activity. If cell proliferation is activated, mutation frequency also may be enhanced with cell cycle acceleration, since gene mutations such as those of *lacI* gene can be transmitted to daughter cells by mitosis. However, our PCNA analysis showed no significant difference between controls, low doses, and high doses of MeIQx. So, the increase of mutation frequency at high-dose MeIQx treatment was not caused by clonal expansion.

Human cancer risk assessment is presently estimated based on extrapolation to low doses of results from animals receiving much higher doses than with normal human exposure. Other researchers have described curves in carcinogenic potential tests at high doses of MeIQx as showing a dose-dependent response (Yamashita *et al.*, 1990) but dose-response curves for carcinogenicity and initiation activity actually differ between high and low exposure (Fukushima *et al.*, 2002, 2003), and Williams *et al.* (2000) also demonstrated the mechanistic basis for nonlinearities and thresholds in rat liver carcinogenesis by genetoxic carcinogens. Taking together, we would argue that genotoxic carcinogens might show threshold, at least practical threshold.

Transgenic animal mutagenesis systems like the Big Blue have been developed to allow measurement of *in vivo* mutagenicity of any organ of interest, although the validity of the *lacI* gene as a human cancer risk marker remains to be confirmed (Suzuki *et al.*, 1996b). Our present study showed *in vivo* mutagenicity to be elevated in the liver, Zymbal gland, and colon, but not in any of the other tissues examined. It should be noted that high-dose treatment with MeIQx was reported to induce hepatocellular carcinomas and squamous cell carcinomas of the Zymbal gland in male F344 rats in long-term animal experiment (Kato *et al.*, 1988). No report has demonstrated tumor occurrence in the colon in animal long-term bioassays as far as we know. However, macroscopically, aberrant crypt foci (ACF), considered to be possible preneoplastic lesions in this organ, have actually been detected in MeIQx-treated F344 rats (Tanakamaru *et al.*, 2001). So our experiments showed *in vivo* mutagenicity and carcinogenicity were completely collaborated at organ level, differing from the previous article showing no direct correlation between mutation frequencies and cancer incidences in mice (Nagao *et al.*, 2001). This discrepancy might be probably due to the differences of species. Further studies were required to disclose these points.

Most genotoxic carcinogens in our surroundings are known to leave specific DNA changes at the individual level, which accumulate to ultimately induce tumors. In order to understand the influence of a genotoxic carcinogen, it is very important to determine the spectrum of DNA damage, as well as the quantity in terms of mutation frequency. Some authors have reported that in the liver of transgenic mice treated with MeIQx, the main mutation is the GC to TA transversion (Ryu *et al.*, 1999). High-dose MeIQx induces *c-k-ras* mutations in codon 12 in the colon of rats, featuring GGT to GAT single base substitutions (Kudo *et al.*, 1991). In zebrafish embryos treated with MeIQx, about 60% of mutations were found to be deletions (Amanuma *et al.*, 2002). In our present study, DNA samples from some of hepatic mutated blue plaque (150 plaques from exposed animals and 2 plaques from controls) were sequenced to examine the nature of the mutations. The mutational spectrum in the liver showed MeIQx to mainly cause mutations at GC pair sites, in accordance with occurrence of bulky adduct at guanine in DNA, such as C8-guanine adduct, N^2-guanine adduct and oxidative stress marker, 8-hydroxyguanosine, although the contribution of these adducts due to MeIQx in the mutation spectrum is not yet known. Furthermore, most mutations involved CpG sites (55.3%), where MeIQx may also induce destablization, producing a bulky intermediate that finally causes mismatch. Our mutational spectrum for *in vivo* mutagenicity, especially involving guanine bases, is completely compatible with *in vitro* mutagenicity in the *lacZ* gene as a reporter of mutations of *E. coli* (Solomon *et al.*, 1996). We concluded that MeIQx produces a very characteristic mutation spectrum, characterized by G deletion *in vivo*.

In conclusion, low doses of the genotoxic carcinogen, MeIQx may show a practical threshold, below which there are no effects, not only for carcinogenic potential but also for *in vivo* mutagenesis. The assumption that the carcinogenic response curve linearly approaches zero at very low doses is not reasonable for assessing human risk.

ACKNOWLEDGMENTS

The author thanks Miss C. Imazato, Miss K. Touma, Miss M. Imanaka, Miss M. Dokoh, and Miss Y. Onishi for expert technical assistance. This research was supported by a grant from the Japan Science and Technology Corporation, included into the Project of Core Research for Evolution Science and Technology (CREST) in Japan.

REFERENCES

Amanuma, K., Tone, S., Saito, H., Shigeoka, T., and Aoki, Y. (2002). Mutational spectra of benzo[a]pyrene and MeIQx in *rpsL* transgenic zebrafish embryos. *Mutat. Res.* **513**, 83–92.

Bailey, G. S., Loveland, P. M., Pereira, C., Pierce, D., Hendricks, J. D., and Groopman, J. D. (1994). Quantitative carcinogenesis and dosimetry in

rainbow trout for aflatoxin B1 and aflatoxicol, two aflatoxins that form the same DNA adduct. *Mutat. Res.* **313,** 25–38.

Cohen, S. M., and Ellwein, L. B. (1990). Cell proliferation in carcinogenesis. *Science* **30,** 1007–1011.

Doll, R., and Peto, R. (1981). The causes of cancer quantitative estimates of avoidable risks of cancer in the United States today. *J. Natl. Cancer Inst.* **66,** 1191–1308.

Fukushima, S., Wanibuchi, H., Morimura, K., Wei, M., Nakae, D., Konishi, Y., Tsuda, H., Uehara, N., Imaida, K., Shirai, T., Tatematsu, M., Tsukamoto, T., Hirose, M., Furukawa, F., Wakabayashi, K., and Totsuka, Y. (2002). Lack of a dose-response relationship for carcinogenicity in the rat liver with low doses of 2-amino-3,8-dimethylimidazo[4,5-*f*]quinoxaline or N-nitrosodiethylamine. *Jpn. J. Cancer Res.* **93,** 1076–1082.

Fukushima, S., Wanibuchi, H., Morimura, K., Wei, M., Nakae, D., Konishi, Y., Tsuda, H., Takasuka, N., Imaida, K., Shirai, T., Tatematsu, M., Tsukamoto, T., Hirose, M., and Furukawa, F. (2003). Lack of initiation activity in rat liver of low doses of 2-amino-3,8-dimethylimidazo[4,5-*f*]quinoxaline. *Cancer Lett.* **191,** 35–40.

IARC (1993). MeIQx, 2-amino-3,8-dimethylimidazo[4,5-f]quinoxaline In *IARC Monographs on the Evaluation of Carcinogenic Risks to Himan-Some Naturally Occurring Substances: Food Items and Constituents, Heterocyclic Aromatic Amines and Mycotoxins,* pp. 211–228. IARC, Lyon, France.

Ito, N., Tsuda, H., Tatematsu, M., Inoue, T., and Tagawa, Y. (1988). Enhancing effect of various Hepatocarcinogens on induction of preneoplastic glutathione *S*-transferase placental form positive foci in rat—an approach for a new medium-term bioassay system. *Carcinogenesis* **9,** 387–394.

Johansson, M. A., and Jagerstad, M. (1994). Occurrence of mutagenic/carcinogenic heterocyclic amines in meat and fish products, including pan residues, prepared under domestic conditions. *Carcinogenesis* **15,** 1511–1518.

Kato, T., Ohgaki, H., Hasegawa, H., Sato, S., Takayama, S., and Sugimura, T. (1988). Carcinogenicity in rats of a mutagenic compound, 2-amino-3,8-dimethylimidazo[4,5-*f*]quinoxaline. *Carcinogenesis* **9,** 71–73.

Kitano, M., Ichihara, T., Matsuda, T., Wanibuchi, H., Tamano, S., Hagiwara, A., Imaoka, S., Funae, Y., Shirai, T., and Fukushima, S. (1998). Presence of a threshold for promoting effects of phenobarbital on diethylnitrosamine-induced hepatic foci in the rat. *Carcinogenesis* **19,** 1475–1480.

Kohler, S. M., Provost, G. S., Fieck. A, Kretz, P. L., Bullock, W. O., Sorge, J. A., Putman, D. L., and Short, J. M. (1991). Spectra of spontaneous and mutagen-induced mutations in the *lacI* gene in transgenic mice. *Proc. Natl. Acad. Sci. U.S.A.* **88,** 7958–7962.

Kudo, M., Ogura, T., Esumi, H., and Sugimura, T. (1991). Mutational activation of *c-Ha-ras* gene in squamous cell carcinomas of rat Zymbal gland induced by carcinogenic heterocyclic amines. *Mol. Carcinog.* **4,** 36–42.

Kushida, H., Wakabayashi, K., Sato, H., Katami, M., Kurosaka, R., and Nagao, M. (1994). Dose-response study of MeIQx carcinogenicity in F344 male rats. *Cancer Lett.* **83,** 31–35.

Langouet, S., Welti, D. H., Kerriguy, N., Fay, L. B., Huynh-Ba, T., Markovic, J., Guengerich, F. P., Guillouzo, A., and Turesky, R. J. (2001). Metabolism of 2-amino-3,8-dimethylimidazo[4,5-*f*]quinoxaline in human hepatocytes: 2-Amino-3-methylimidazo[4,5-*f*]quinoxaline-8-carboxylic acid is a major detoxification pathway catalyzed by cytochrome P450 1A2. *Chem. Res. Toxicol.* **14,** 211–221.

Lutz, W. K. (1998). Dose-response relationships in chemical carcinogenesis: Superposition of different mechanisms of action, resulting in linear-nonlinear curves, practical thresholds, J-shapes. *Mutat. Res.* **405,** 117–124.

Lutz, W. K. (2001). Susceptibility differences in chemical carcinogenesis linearize the dose-response relationship: Threshold doses can be defined only for individuals. *Mutat. Res.* **482,** 71–76.

Maier, P., and Schawalder, H. P. (1988). Hepatocarcinogens induce gene mutations in rats in fibroblast-like cells from a subcutaneous granulation tissue. *Carcinogenesis* **9,** 1363–1368.

Nagao, M., Ochiai, M., Okochi, E., Ushijima, T., and Sugimura, T. (2001). LacI transgenic animal study: Relationships among DNA-adduct levels, mutant frequencies and cancer incidences. *Mutat. Res.* **477,** 119–124.

Nishikawa, A., Furukawa, F., Kasahara, K., Lee, I. S., Suzuki, T., Hayashi, M., Sofuni, T., and Takahashi, M. (1997). Comparative study on organ-specificity of tumorigenicity, mutagenicity and cell proliferative activity induced by dimethylnitrosamine in Big Blue mice. *Cancer Lett.* **117,** 143–147.

Oesch, F., Herrero, M. E., Hengstler, J. G., Lohmann, M., and Arand, M. (2000). Metabolic detoxification: Implications for thresholds. *Toxicol. Pathol.* **28,** 382–387.

Okochi, E., Watanabe, N., Shimada, Y., Takahashi, S., Wakazono, K., Shirai, T., Sugimura, T., Nagao, M., and Ushijima, T. (1999). Preferential induction of guanine deletion at 5′-GGGA-3′ in rat mammary glands by 2-amino-1-methyl-6-phenylimidazo[4,5-*b*]pyridine. *Carcinogenesis* **20,** 1933–1938.

Preussmann, R. (1980). The problem of thresholds in chemical carcinogenesis-some views on threoretical and practical aspects. *Cancer Res. Clin. Oncol.* **97,** 1–14.

Rogers, B. J., Provost, G. S., Young, R. R., Putman, D. L., and Short, J. M. (1995). Intralaboratory optimization and standardization of mutant screening conditions used for a *lambda/lacI* transgenic mouse mutagenesis assay (I). *Mutat. Res.* **327,** 57–66.

Ryu, D. Y., Pratt, V. S., Davis, C. D., Schut, H. A., and Snyderwine, E. G. (1999). In vivo mutagenicity and hepatocarcinogenicity of 2-amino-3,8-dimethylimidazo[4,5-*f*]quinoxaline (MeIQx) in bitransgenic *c-myc/lambda lacZ* mice. *Cancer Res.* **59,** 2587–2592.

Solomon, M. S., Morgenthaler, P. M., Turesky, R. J., and Essigmann, J. M. (1996). Mutational and DNA binding specificity of the carcinogen 2-amino-3, 8-dimethylimidazo[4,5-*f*]quinoxaline. *J. Biol. Chem.* **271,** 18368–18374.

Sugimura, T. (1986). Studies on environmental chemical carcinogenesis in Japan. *Science* **233,** 312–318.

Suzuki, T., Hayashi, M., Ochiai, M., Wakabayashi, K., Ushijima, T., Sugimura, T., Nagao, M., and Sofuni T. (1996a). Organ variation in the mutagenicity of MeIQ in Big Blue *lacI* transgenic mice. *Mutat Res.* **369,** 45–49.

Suzuki, T., Itoh, T., Hayashi, M., Nishikawa, Y., Ikezaki, S., Furukawa, F., Takahashi, M., and Sofuni, T. (1996b). Organ variation in the mutagenicity of dimethylnitrosamine in Big Blue mice. *Environ. Mol. Mutagen.* **28,** 348–353.

Tanakamaru, Z., Mori, I., Nishikawa, A., Furukawa, F., Takahashi, M., and Mori, H. (2001). Essential similarities between spontaneous and MeIQx-promoted aberrant crypt foci in the F344 rat colon. *Cancer Lett.* **172,** 143–149.

Troxel, C. M., Reddy, A. P., O'Neal, P. E., Hendricks, J. D., and Bailey, G. S. (1997). In vivo aflatoxin B1 metabolism and hepatic DNA adduction in zebrafish. *Toxicol. Appl. Pharmacol.* **143,** 213–220.

Truhaut, R. (1979). An overview of the problem of thresholds for chemical carcinogens. *IARC Sci. Publ.* **25,** 191–202.

Ushijima, T., Hosoya, Y., Suzuki, T., Sofuni, T., Sugimura, T., and Nagao, M. (1995). A rapid method for detection of mutations in the *lacI* gene using PCR-single strand conformation polymorphism analysis: Demonstration of its high sensitivity. *Mutat. Res.* **334,** 283–292.

Vogelstein, B., and Kinzler, K. W. (1993). The multistep nature of cancer. *Trends Genet.* **9,** 138–141.

Williams, G. M., Iatropoulos, M. J., and Jeffrey, A. M. (2000). Mechanistic basis for nonlinearities and thresholds in rat liver carcinogenesis by the DNA-reactive carcinogens 2-acetylaminofluorene and diethylnitrosamine. *Toxicol. Pathol.* **28,** 388–395.

Wolff, S. (1998). The adaptive response in radiobiology: Evolving insights and implications. *Environ. Health Perspect.* **106,** 277–283.

Yamashita, K., Adachi, M., Kato, S., Nakagama, H., Ochiai, M., Wakabayashi, K., Sato, S., Nagao, M., and Sugimura, T. (1990). DNA adducts formed by 2-amino-3,8-dimethylimidazo[4,5-*f*]quinoxaline in rat liver: Dose-response on chronic administration. *Jpn. J. Cancer Res.* **81,** 470–476.

Journal of Andrology, Vol. 25, No. 1, January/February 2004

Zinc and Metallothionein Levels and Expression of Zinc Transporters in Androgen-Independent Subline of LNCaP Cells

KAZUHIRO IGUCHI,* TAKASHI OTSUKA,* SHIGEYUKI USUI,* KENICHIRO ISHII,† TAKEHISA ONISHI,‡ YOSHIKI SUGIMURA,‡ AND KAZUYUKI HIRANO*

*From the *Laboratory of Pharmaceutics, Gifu Pharmaceutical University, Mitahora-higashi, Gifu, Japan; †Department of Urologic Surgery, Vanderbilt University Medical Center, Nashville, Tennessee; and the ‡Department of Urology, Mie University School of Medicine, Edobashi, Tsu, Mie, Japan.*

ABSTRACT: Zinc levels in the prostate have been reported to be associated with the development and progression of malignant prostate cells. To investigate the reason why the zinc content decreases during the progression of prostate cancer to an androgen-independent state, we compared the expression levels of metallothionein and zinc transporters between androgen-responsive LNCaP cells and its androgen-independent subline, AIDL cells. AIDL cells showed lower zinc levels than LNCaP cells and comparable levels of androgen receptor expression to LNCaP cells, consistent with some clinical aspects of androgen-independent prostatic cancer. AIDL cells exhibited a lower expression of zinc transporter 1 (ZnT1) and higher expression of ZnT3 than LNCaP cells. The content of metallothionein, which is a major zinc-binding protein, was significantly lower in AIDL cells than in LNCaP cells. Furthermore, the expression of ZnT3 mRNA was decreased by incubating LNCaP cells in medium containing hormone-stripped fetal calf serum and increased by addition of synthetic androgen R1881 to the medium, whereas the intracellular zinc levels were not affected under these conditions. These findings suggest that factors such as ZnT1 and metallothioneins other than ZnT3 are associated with the low intracellular zinc content in AIDL cells.

Key words: Hormone-refractory, metallothionein, ZnT1, ZnT3.
J Androl 2004;25:154–161

High concentrations of zinc, an essential nutrient for most cells and tissues, are known to be retained in the prostate gland and secreted into the seminal plasma (Mawson and Fischer, 1951, 1952, 1953). A deficiency of zinc leads to male hypogonadism accompanied by inhibition of sperm formation and a lack of secondary sex characteristics (Prasad, 1983, 1985). Zinc has also been suggested to have an antibacterial function in seminal plasma (Fair et al, 1976). Moreover, prostatic zinc has been found to control prostatic epithelial cell growth through inhibition of mitochondrial aconitase activities, cell cycle arrest, and induction of cell detachment (Costello and Franklin, 1981; Costello et al, 1997; Iguchi et al, 1998; Liang et al, 1999). Recently, zinc in prostate cancer has been reported to regulate the metastasis through the inhibition of the enzymatic activity of aminopeptidase N and urokinase-type plasminogen activator (Ishii et al, 2001). Thus the physiological functions of zinc in the prostate have been gradually revealed.

Correspondence to: Dr Kazuyuki Hirano, Laboratory of Pharmaceutics, Gifu Pharmaceutical University, 5-6-1 Mitahora-higashi, Gifu 502-8585, Japan (e-mail: hirano@gifu-pu.ac.jp).

Received for publication May 7, 2003; accepted for publication August 13, 2003.

Possible relations between changes of zinc content in the prostate and prostatic diseases have been investigated. The zinc level in prostate cancer was observed to decrease to that detected in nonprostate tissues (Gyorkey et al, 1967; Ogunlewe and Osegbe, 1989). Zinc levels in seminal plasma of patients with bacterial prostatitis or sterility were also reported to be consistently lower than those in healthy subjects (Fair et al, 1976; Fair and Parrish, 1981). High levels of zinc have been found in the prostate grand with benign prostatic hyperplasia compared with the normal prostate (Gyorkey et al, 1967; Ogunlewe and Osegbe, 1989). Although functional disorder of zinc homeostasis seems to be associated with prostatic disease, it is unclear whether diseases cause the disruption of zinc homeostasis or vice versa.

Since the growth and progression of prostate cancer are initially androgen-dependent, androgen ablation therapies have been the standard treatment for prostate cancer (Huggins and Hodges, 1941). Hormone ablation therapy only causes a temporary regression of prostate cancer; however, the progression of an androgen-dependent prostate cancer to an androgen-independent state is a well-established phenomenon (Emmett et al, 1960). In androgen-independent prostate cancer, zinc levels have been

found to be much lower than those in an androgen-dependent state (Shiina et al, 1996a,b), but little information is available as to why zinc content decreases during the progression of prostate cancer to a hormone-independent state after androgen withdrawal therapy.

Many transporters and metal-binding proteins regulating zinc homeostasis have been identified in mammals. Natural resistance-associated macrophage protein 2 (Nramp2) is a metal ion transporter that imports a variety of metal ions such as Fe, Zn, Cd, and Cu from the extracellular environment into cells (Gunshin et al, 1997). Zinc transporter 1 (ZnT1) is a zinc transporter responsible for zinc efflux across the plasma membranes to prevent zinc toxicity (Palmiter and Findley, 1995). Zinc transporter 2 (ZnT2) is involved in zinc uptake into vesicles (endosome/lysosome compartment) in intestine, kidney, and testis (Palmiter et al, 1996a). Zinc transporter 3 (ZnT3) is expressed in the brain and is responsible for the accumulation of zinc in synaptic vesicles (Palmiter et al, 1996b). Zinc transporter 4 (ZnT4) is associated with zinc efflux or compartmentalization in the mammary gland, and is essential for regulating the zinc content of milk (Huang and Gitschier, 1997; Murgia et al, 1999). Zn-regulated transporter/Fe-regulated transporterlike proteins (ZIP) are suggested to be involved in zinc influx across the plasma membranes because forced expression of these transporters in mammalian cells increased their zinc uptake (Gaither and Eide, 2000). Nramp2, ZnT1, and ZnT4 are ubiquitously expressed in most tissues, whereas ZnT2 and ZnT3 display tissue-restricted expression in mammals. Metallothioneins are a major family of zinc-binding proteins and are well known to play an important role in zinc uptake, distribution, storage, and release (Cousins, 1985).

In the present study, to clarify the role of zinc in the progression of prostate cancer to an androgen-independent state, we investigated expression levels of zinc transporters and metallothionein in androgen-independent LNCaP (AIDL) cells and native LNCaP cells. Elucidation of the zinc retention system in the prostate will be useful for investigation of prostatic diseases.

Materials and Methods

Cell Culture

Androgen-responsive LNCaP cells were purchased from American Type Culture Collection (Rockville, Md), and androgen-independent LNCaP cells (AIDL) were established by Dr. T. Ohnishi at Mie University Faculty of Medicine. The AIDL cells were established from LNCaP cells by maintaining in phenol red-free RPMI-1640 medium (Sigma, St. Louis, Mo) with 2% charcoal-stripped fetal calf serum (CS-FCS) over 2 years (Kokontis et al, 1994; Onishi et al, 2000, 2001). LNCaP and AIDL cells were cultured in phenol red-free RPMI-1640 medium with 10% FCS (LNCaP) or 2% CS-FCS (AIDL), respectively.

Cell Proliferation

Cell proliferation was evaluated by measurement of the fluorescence intensity in the presence of alamar blue (Wako, Osaka, Japan) (Pagé et al, 1993). Cells were seeded in 96-well multidishes (Sumilon, Tokyo, Japan) at a density of 1×10^4 cells/well in phenol red-free RPMI-1640 medium supplemented with 2% CS-FCS, and after 1 day, androgen agonist R1881 (NEN Life Science, Boston, Mass) was added to the culture medium. After 72 h, alamar blue solution was added to the medium, and the plates were incubated for 4 hours. The fluorescence intensity was measured using a Cytofluor 2350 with excitation and emission wavelengths at 530 nm and 590 nm, respectively.

Zinc Assay

Zinc concentration was measured using 2-(5-bromo-2-pyridylazo)-5-(*N*-propyl-*N*-sulfopropylamino)phenol disodium salt dihydrate (5-Br-PAPS, Dojindo Laboratory, Kumamoto, Japan) (Yamashita et al, 1996). Briefly, cells were cultured in 90-mm dishes (Sumilon) in phenol red-free RPMI-1640 medium supplemented with 2% CS-FCS for 3 days. After being washed with phosphate-buffered saline, the cells were pelleted, treated with 10% trichloroacetic acid on ice for 15 minutes, and centrifuged at 4°C for 10 minutes. The resulting supernatant was incubated with 0.08 nM 5-Br-PAPS and 29 mM salicyladoxime for 10 minutes at room temperature. The absorbance of the mixture was measured at 570 nm with a microplate reader.

Metallothionein Assay

The total amount of metallothionein was determined by the cadmium-saturation assay (Onosaka et al, 1978). Briefly, cells were incubated in phenol red-free RPMI-1640 medium supplemented with 2% CS-FCS for 3 days. The cells were collected, resuspended in 10 mM Tris-HCl (pH 7.4), and sonicated. The cell lysate was then centrifuged at 105 000 × *g* at 4°C for 60 minutes. The resulting supernatant was incubated with 0.2 μg of Cd^{2+} for 10 minutes at room temprature. After removal of unbound Cd^{2+} by using hemoglobin as a chelator, Cd^{2+} bound to metallothionein was measured with an atomic adsorption spectrophotometer (Shimadzu AA-6500).

Semiquantitative Reverse Transcriptase Polymerase Chain Reaction

Total RNA was isolated using TRIzol reagent (Invitrogen, Carlsbad, Cal) according to the manufacturer's instructions. Extracted RNA was dissolved in diethylpyrocarbonate-treated water and quantified by measuring the absorbance at 260 nm. Aliquots of 5 μg of total RNA were used to synthesize the first-strand complementary DNA with SuperScript II (Invitrogen) and subjected to polymerase chain reaction (PCR) amplification with the oligonucleotide primers listed in Table 1 using a thermal cycler. The optimal PCR conditions were determined as the amount of amplification product in proportion to that of input RNA. PCR was performed under the following conditions: 26 cycles of 1 minute at 94°C, 1 minute at 57°C, and 1 minute at 72°C for androgen receptor (AR); 24 cycles of 1 minute at 94°C, 1 minute

Sequences of oligonucleotide primers for PCR

Gene name	Sequence	Product size (bp)
AR	Sense: 5'-GCAGGAAGCAGTATCCGAAG-3'	302
	Antisense: 5'-CGCTGTCGTCTAGCAGAGAA-3'	
PSA	Sense: 5'-GAGGTCCACACACTGAAGTT-3'	217
	Antisense: 5'-CCTCCTGAAGAATCGATTCCT-3'	
ZnT1	Sense: 5'-TGTGAACTTGCCTGCAGAAC-3'	158
	Antisense: 5'-GCTTTAGTCCTCCTGGGCTT-3'	
ZnT3	Sense: 5'-TGCAGAGGCAACATGGTAAG-3'	135
	Antisense: 5'-ATCCTCATGGAAGGTACCCC-3'	
ZnT4	Sense: 5'-GTGAAAGCCAGGTTGACCAT-3'	464
	Antisense; 5'-TGGTTAGCTTCACACCCAGA-3'	
Nramp2	Sense: 5'-AACCCAGCCAGAGCCAGGTA-3'	391
	Antisense: 5'-CCCCCTTTGTAGATGTCCAC-3'	
ZIP1	Sense: 5'-GTCCTGGTGATGGAGCAGAT-3'	398
	Antisense: 5'-CCGATGCCTAGAGGTGTCAT-3'	
ZIP3	Sense: 5'-CAGTCCCATGTCATGCAGAG-3'	214
	Antisense: 5'-GGAGCTCAAGGAACAGGTCA-3'	
G3PDH	Sense: 5'-TGAAGGTCGGAGTCAACGGATTTGGT-3'	983
	Antisense: 5'-CATGTGGGCCATGAGGTCCACCAC-3'	

at 54°C, and 1 minute at 72°C for prostate-specific antigen (PSA); 26 cycles of 1 minute at 94°C, 1 minute at 55°C, and 1 minute at 72°C for ZnT1 and ZnT4; 28 cycles of 1 minute at 94°C, 1 minute at 55°C, and 1 minute at 72°C for ZnT3 and ZIP1; 25 cycles of 1 minute at 94°C, 1 minute at 60°C, and 1 minute at 72°C for Nramp2; 28 cycles of 1 minute at 94°C, 1 minute at 62°C, and 1 minute at 72°C for ZIP3; 23 cycles of 45 seconds at 94°C, 45 seconds at 60°C, and 2 minutes at 72°C for glyceraldehyde-3-phosphate dehydrogenase (G3PDH). G3PDH served as an internal RNA control to allow comparison of RNA levels among different specimens. After PCR, the reaction products were resolved on 1.75 % agarose gels and visualized with ethidium bromide.

Protein Assay

The protein concentration was determined by Lowry assay using bovine serum albumin as a standard (Lowry et al, 1951).

Results

Characterization of AIDL and LNCaP Cells

AIDL cells, which can grow well in the absence of androgen, are an LNCaP subline derived by continuous passaging in hormone-depleted medium. The viability of LNCaP cells incubated for 72 hours in CS-FCS-containing medium was approximately half of that in FCS-containing medium, whereas the viability of AIDL cells incubated in CS-FCS-containing medium was 1.3-fold of that in FCS-containing medium (data not shown). A previous study showed that the activities of mitogen-activated protein kinases were higher in AIDL cells than in LNCaP cells (Onishi et al, 2001). Moreover, to ascertain that AIDL cells exhibit features of androgen-independent prostate cancer, androgen responsiveness of cell proliferation, AR and PSA expressions, and intracellular zinc levels were investigated. Androgen responsiveness of these cells was assessed by measuring the effect of synthetic androgen R1881 on cell growth. As shown in Figure 1A, the proliferation of LNCaP cells was stimulated by R1881 in a dose-dependent manner but no significant effect on the growth of AIDL cells was observed. The expression of AR in AIDL cells showed approximately the same as that in LNCaP cells; however, PSA expression was not detected in AIDL cells (Figure 1B). Therefore, we next assessed the transcriptional activity of AR in AIDL cells by measuring induction of PSA mRNA in response to R1881 treatment. As shown in Figure 1C, increased expression of PSA was observed after 8–16 days of incubation in R1881-stimulated AIDL cells, whereas the same treatment increased the expression after 1 day in LNCaP cells. These results suggest that the androgen-independent behavior in AIDL cells possibly involves an alteration of AR function or an abnormality in AR signal transduction pathway. We also determined zinc levels in AIDL and LNCaP cells. As shown in Figure 2, the zinc levels in AIDL cells were significantly lower than those in LNCaP cells. Thus, AIDL cells were judged to retain some features observed in the androgen-independent prostate cancer.

Expression of Zinc Transporters and Metallothionein in AIDL and LNCaP Cells

Zinc homeostasis in eukaryotic cells is believed to be controlled by zinc uptake, elimination, and intracellular sequestration, which are regulated by the expression levels of various zinc transporters and the major zinc-binding protein metallothionein (Beyersmann and Haase, 2001). To determine factors involved in the decrease of zinc con-

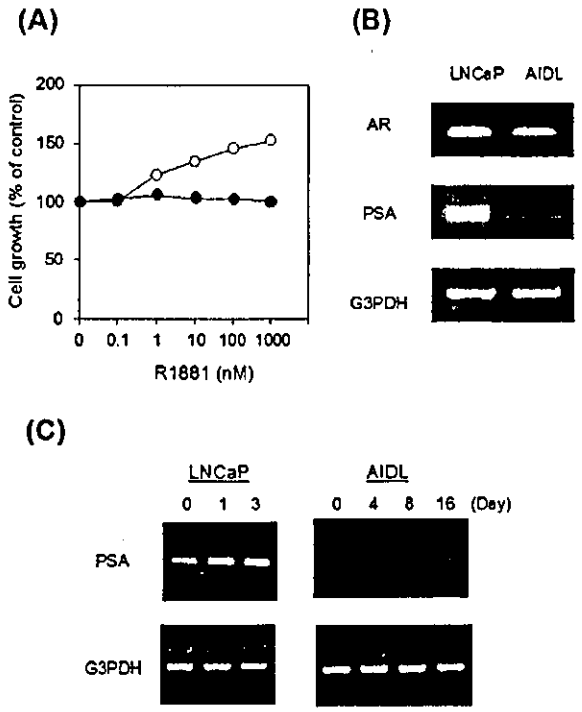

Figure 1. Androgen-independent behavior of AIDL cells. (A) LNCaP (O) and AIDL cells (●) (1×10^4 cells/well) were grown in phenol red-free RPMI-1640 supplemented with 2% fetal calf serum (FCS), 2% charcoal-stripped (CS)-FCS, or 2% CS-FCS containing 100 nM R1881 for 72 h. Cell proliferation was examined by alamar blue assay. (B) Total RNA was isolated from LNCaP and AIDL cells grown in phenol red-free RPMI-1640 supplemented with 2% CS-FCS for 3 d, and subjected to reverse transcriptase polymerase chain reaction (RT-PCR) with the specific primer sets. The products were resolved on 1.75% agarose gels and visualized with ethidium bromide. (C) LNCaP and AIDL cells were grown in phenol red-free RPMI-1640 supplemented with 2% CS-FCS for 3 d, and then 100 nM R1881 was added to the medium. R1881-containing medium was replaced every 3 d. Total RNA was isolated at the indicated times and subjected to RT-PCR analysis. The products were resolved on 1.75% agarose gels and visualized with ethidium bromide.

tent in androgen-independent prostatic cancer, we next tried to examine the expression of zinc transporters and metallothionein contents in LNCaP and AIDL cells. As shown in Figure 3, the levels of ZnT1 and ZnT3 mRNAs were approximately 1.5-fold and 4-fold higher in AIDL cells than LNCaP cells. The expressions of ZnT4, Nramp2, ZIP1, and ZIP3 showed no significant differences between them. Moreover, as shown in Figure 4, the levels of metallothionein in AIDL cells were approximately threefold lower than those in LNCaP cells.

Effect of R1881 on Intracellular Zinc and Metallothionein Levels, and Expressions of Zinc Transporters

Since AIDL cells were generated by long-term culture of androgen-responsive LNCaP cells in the medium containing hormone-stripped serum, the decrease in intracellular zinc and metallothionein and the increase in ZnT1 and

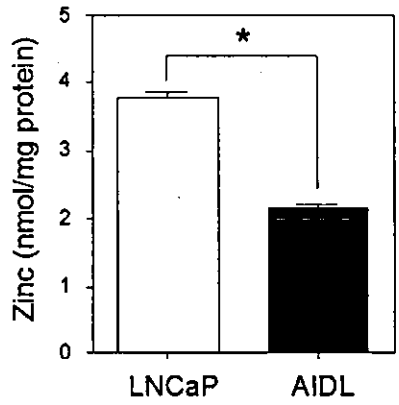

Figure 2. Zinc levels in LNCaP and AIDL cells. LNCaP and AIDL cells were grown in phenol red-free RPMI-1640 supplemented with 2% charcoal-stripped fetal calf serum (CS-FCS) for 3 d, and zinc levels were determined by the method described in *Materials and Methods*. Values represent the means ± SD from 3 incubations. * indicates $P < .001$ vs LNCaP (Student's *t*-test).

ZnT3 expressions in AIDL cells may be mediated by androgenic regulation. Therefore, we next tried to assess the effects of androgen-sufficient or -deficient conditions on zinc accumulation, metallothionein levels, and ZnTs expressions in LNCaP cells. As shown in Figure 5, the expression of ZnT3 mRNA in LNCaP cells was decreased by the treatment with 100 nM R1881, whereas slightly increased by hormone ablation, suggesting that androgen negatively regulated ZnT3 expression. The altered expressions of ZnT3 were seen in androgen-responsive LNCaP cells but not in androgen-independent AIDL cells, supporting the idea that the expression of ZnT3 was regulated by androgen (Figure 5C). The expressions of the other zinc transporters including ZnT1 were not observed to be androgen regulated. The zinc and metallothionein levels were also not affected by treatment of LNCaP cells with either R1881 or androgen ablation (Figure 6).

Discussion

To mimic androgen ablation therapy for the treatment of prostate cancer, we chronically cultured androgen-responsive LNCaP cells in androgen-reduced conditions, generating an androgen-independent derivative AIDL, which retained limited hormone-responsive proliferation (Onishi et al, 2000, 2001). Although AIDL cells retained a similar level of AR mRNA expression, transcriptional activity of AR in AIDL cells was significantly lower than that in LNCaP cells, suggesting that AIDL cells exhibit an AR abnormality such as AR gene mutation. These findings confirm some clinical observations of hormone-refractory prostate cancer. Moreover, AIDL cells showed much lower zinc levels compared with native LNCaP cells, consis-

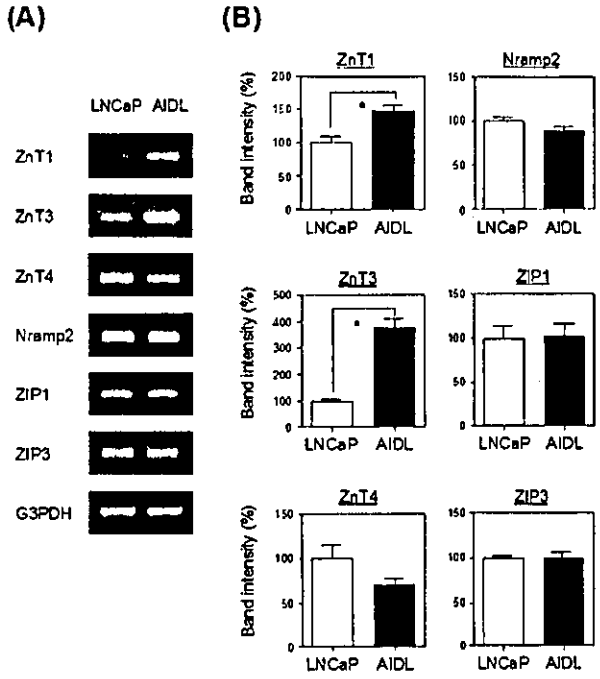

Figure 3. Reverse transcriptase polymerase chain reaction (RT-PCR) analysis of zinc transporter mRNA expression in LNCaP and AIDL cells. (A) Total RNA was isolated from LNCaP and AIDL cells grown in phenol red-free RPMI-1640 supplemented with 2% charcoal-stripped fetal calf serum for 3 d, and subjected to RT-PCR analysis. The products were resolved on 1.75% agarose gels and visualized with ethidium bromide. (B) Band intensity was quantified using the National Institutes of Health Image program. The intensities were normalized with glyeraldehyde-3-phosphate dehydrogenase as a standard and expressed as a percentage of the value from LNCaP cells. Values represent the means ± SD from 3 different experiments. * indicates $P < .01$ vs LNCaP (Student's *t*-test).

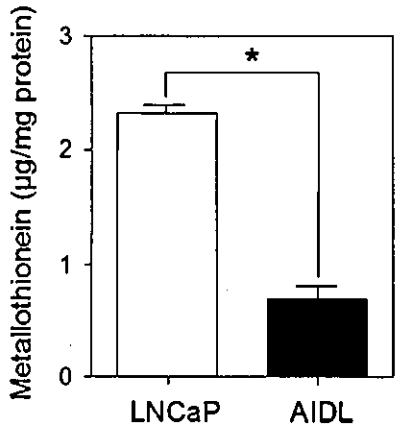

Figure 4. Metallothionein levels in LNCaP and AIDL cells. The cells were grown in phenol red-free RPMI-1640 supplemented with 2% charcoal-stripped fetal calf serum for 3 d, and metallothionein levels were determined by cadmium saturation assay. Values represent the means ± SD from 3 incubations. * indicates $P < .001$ vs LNCaP (Student's *t*-test).

tent with the clinical evidence that zinc levels in androgen-independent prostate cancer was much lower than those in an androgen-dependent state (Shiina et al, 1996a,b). Thus, AIDL cells seem to be useful for investigating the zinc retention system in hormone-refractory prostate cancer.

In the present study, we analyzed the expression of zinc transporters and metallothionein content in LNCaP and AIDL cells to obtain clues about the reason why the zinc content decreases during the progression of prostatic cancer. Our experiments revealed that ZnT1 and ZnT3 mRNA expressions were higher and metallothionein levels were lower in AIDL cells than in native LNCaP cells. Since ZnT3 was found abundantly and has been believed to play a crucial role in the regulation of zinc transport into vesicles in mammalian brain (Cole et al, 1999; Lee et al, 2000), the increased expression of ZnT3 would affect the cellular localization of zinc but not affect the total amount of intracellular zinc. In fact, the R1881-treated LNCaP cells showed no significant changes of zinc content, although the expression of ZnT3 mRNA was decreased in the cells. These results suggest that the decrease in the expression level of ZnT3 mRNA does not reflect the change in the intracellular zinc content in LNCaP cells.

ZnT-1 transports zinc out of cells and has been suggested to play a key role in cellular zinc homeostasis (Palmiter et al, 1995). Increased cellular zinc content induces ZnT1 gene expression to efflux zinc from cells (Palmiter et al, 1995; McMahon and Cousins, 1998). The regulation of ZnT1 mRNA expression was found to be mediated by binding of metal response element-binding transcription factor-1 to metal response elements (MREs) sequence present in the ZnT1 promoter region (Langmade et al, 2000; Andrews, 2001). These findings led us to speculate that decreased cellular zinc content in AIDL cells may lead to a decrease in ZnT1 expression. However, the expression was observed to be higher than in LNCaP cells. The reason why the expression of ZnT1 increased in AIDL cells is unknown, but from the viewpoint of its function as effluxing zinc, the increased ZnT1 expression may result in the low intracellular zinc content in the cells.

Since metallothionein acts as a zinc store in the cell and its gene is also transcriptionally regulated by intracellular zinc thorough cis-acting MREs (Andrews, 2001), the low level of zinc in AIDL cells could be closely related to the low expression of metallothionein observed in these cells. However, the reason for the decreased expression of metallothionein in AIDL cells is probably more complex since its expression is also regulated by various stress factors, including glucocorticoids, cytokines, and reactive oxygen species (Palmiter, 1998). Therefore, the low level of metallothionein in AIDL cells,